

NAVAL POSTGRADUATE SCHOOL

Monterey, California

AD-A216 552



THESIS

DTIC
ELECTE
JAN 11 1990
S E D

OPTIMIZING SUPERPLASTIC RESPONSE IN
NAVALITE,
A LITHIUM CONTAINING
ALUMINUM-MAGNESIUM ALLOY

by

Alden P. Chester, III

June 1989

Thesis Advisor

T.R. McNelley

Approved for public release; distribution is unlimited.

90 01 10 146

Unclassified

security classification of this page

REPORT DOCUMENTATION PAGE

1a Report Security Classification Unclassified			1b Restrictive Markings		
2a Security Classification Authority			3 Distribution Availability of Report Approved for public release; distribution is unlimited.		
2b Declassification Downgrading Schedule					
4 Performing Organization Report Number(s)			5 Monitoring Organization Report Number(s)		
6a Name of Performing Organization Naval Postgraduate School		6b Office Symbol (if applicable) 34	7a Name of Monitoring Organization Naval Postgraduate School		
6c Address (city, state, and ZIP code) Monterey, CA 93943-5000			7b Address (city, state, and ZIP code) Monterey, CA 93943-5000		
8a Name of Funding Sponsoring Organization		8b Office Symbol (if applicable)	9 Procurement Instrument Identification Number		
8c Address (city, state, and ZIP code)			10 Source of Funding Numbers		
			Program Element No	Project No	Task No
			Work Unit Accession No		
11 Title (include security classification) OPTIMIZING SUPERPLASTIC RESPONSE IN NAVALITE, A LITHIUM CONTAINING ALUMINUM-MAGNESIUM ALLOY					
12 Personal Author(s) Alden P. Chester.III					
13a Type of Report Master's Thesis		13b Time Covered From To		14 Date of Report (year, month, day) June 1989	
				15 Page Count 72	
16 Supplementary Notation The views expressed in this thesis are those of the author and do not reflect the official policy or position of the Department of Defense or the U.S. Government.					
17 Cosati Codes			18 Subject Terms (continue on reverse if necessary and identify by block number)		
Field	Group	Subgroup	word processing, Script, GML, text processing.		
19 Abstract (continue on reverse if necessary and identify by block number) Superplastic ductilities up to 428 percent have been attained during research into thermomechanical processing of $\text{Al-2.70Mg-2.04Li-0.50Cu-0.13Zr}$ (compositions in wt.pct.; alloy composition corresponding to NAVALITE). Variation in dislocation density induced by means of warm rolling at a series of temperatures below the discontinuous recrystallization temperature were expected to significantly affect the superplastic response by further grain size refinement. Experimental results indicate no beneficial enhancement in ductilities associated with rolling below 250 °C. Consistent elongations in the 400 percent range during this initial evaluation of the NAVALITE alloy indicates further investigation of superplastic response is warranted.					
20 Distribution Availability of Abstract <input checked="" type="checkbox"/> unclassified unlimited <input type="checkbox"/> same as report <input type="checkbox"/> DTIC users			21 Abstract Security Classification Unclassified		
22a Name of Responsible Individual T.R. McNelley			22b Telephone (include Area code) (408) 646-2589		22c Office Symbol 69MC

DD FORM 1473, 84 MAR

83 APR edition may be used until exhausted
All other editions are obsolete

security classification of this page

Unclassified

Approved for public release; distribution is unlimited.

Optimizing Superplastic Response in NAVALITE,
a Lithium Containing Aluminum-Magnesium Alloy

by

Alden P. Chester, III
Lieutenant, United States Navy
B.S.I.M., Purdue University, 1978

Submitted in partial fulfillment of the
requirements for the degree of

MASTER OF SCIENCE IN MECHANICAL ENGINEERING

from the

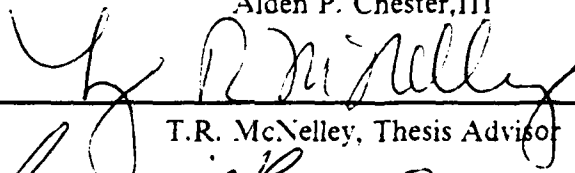
NAVAL POSTGRADUATE SCHOOL
June 1989

Author:

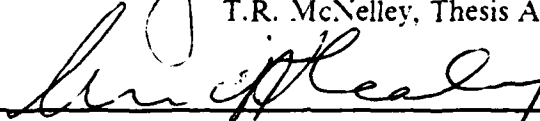


Alden P. Chester, III

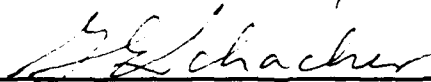
Approved by:



T.R. McNelley, Thesis Advisor



Anthony J. Healey, Chairman,
Department of Mechanical Engineering



Gordon E. Schacher,
Dean of Science and Engineering

ABSTRACT

Superplastic ductilities up to 428 percent have been attained during research into thermomechanical processing of Al-2.70Mg-2.04Li-0.50Cu-0.13Zr (compositions in wt.pct.; alloy composition corresponding to NAVALITE). Variation in dislocation density induced by means of warm rolling at a series of temperatures below the discontinuous recrystallization temperature were expected to significantly affect the superplastic response by further grain size refinement. Experimental results indicate no beneficial enhancement in ductilities associated with rolling below 250 °C. Consistent elongations in the 400 percent range during this initial evaluation of the NAVALITE alloy indicates further investigation of superplastic response is warranted.

Accession For	
NTIS	<input checked="checked" type="checkbox"/>
DTIC TAB	<input type="checkbox"/>
Unannounced	<input type="checkbox"/>
Justification	
By	
Distribution/	
Availability Codes	
Dist	Avail and/or Special
A-1	



TABLE OF CONTENTS

I. INTRODUCTION	1
II. BACKGROUND	3
A. ALLOYS OF ALUMINUM	3
1. Al-Mg	3
2. Al-Mg-Li	3
3. NAVALITE	4
B. CONDITIONS FOR SUPERPLASTICITY	5
1. Grain Size	5
2. Second Phase	5
3. Grain Boundary Sliding	5
4. Strain Rate Sensitivity and Phenomenological Aspects	6
5. Thermomechanical Processing	6
III. EXPERIMENTAL PROCEDURE	8
A. CASTING AND SECTIONING	8
B. SOLUTION TREATMENT STUDY	8
C. THERMOMECHANICAL PROCESSING	8
D. TENSILE TESTING	11
E. DATA REDUCTION	11
F. OPTICAL MICROSCOPY	13
IV. RESULTS AND DISCUSSION	14
A. SOLUTION TREATMENT STUDY	14
B. ROLLING AT 300°C	14
C. VARIATION IN TMP ROLLING TEMPERATURES	18
D. INTERPRETATION OF RESULTS	28
V. CONCLUSIONS	33
VI. RECOMMENDATIONS FOR FURTHER STUDY	34

APPENDIX A. DUCTILITIES (PCT. ELONG.) OF TMP C, D AND E	35
APPENDIX B. TRUE STRESS VS. TRUE STRAIN CURVES	36
APPENDIX C. STRAIN-RATE SENSITIVITY FOR TMP A, C, D, AND E ..	51
APPENDIX D. VARIATION OF STRAIN-RATE SENSITIVITY FOR TMP A, C, D, AND E	55
LIST OF REFERENCES	59
INITIAL DISTRIBUTION LIST	61

LIST OF TABLES

Table 1.	SOLUTION TREATMENT STUDY	8
Table 2.	THERMAL MECHANICAL PROCESSING REGIMES	10
Table 3.	ROLLING SCHEDULE	12
Table 4.	DUCTILITY (% ELONG.) OF MATL. PROCESSED WITH TMP A	17
Table 5.	DUCTILITY (% ELONG.) OF MATL. PROCESSED WITH TMP B	18
Table 6.	DUCTILITY (% ELONG.) OF MATL. PROCESSED WITH TMP C	35
Table 7.	DUCTILITY (% ELONG.) OF MATL. PROCESSED WITH TMP D	35
Table 8.	DUCTILITY (% ELONG.) OF MATL. PROCESSED WITH TMP E	35

LIST OF FIGURES

Figure 1.	Aluminum Corner of the Al-Mg-Li Phase Diagram at 460°C	4
Figure 2.	TMP Employed on Al-10Mg, Al-10Mg-1Li	7
Figure 3.	TMP Logic Chart	9
Figure 4.	TMP for Sample A	10
Figure 5.	TMP for sample B	11
Figure 6.	TMP for sample E	12
Figure 7.	Tensile Test Specimen Drawing	13
Figure 8.	Cast NAVALITE billet #606170A(N2)	15
Figure 9.	NAVALITE casting after solution treatment #3	16
Figure 10.	NAVALITE after solution treatment and forging	17
Figure 11.	TMP B - Percent elongation vs. temperature	19
Figure 12.	TMP B - Percent elongation vs. strain rate	20
Figure 13.	Ductility (% Elong.) of Material processed with TMP A	21
Figure 14.	Ductility (% Elong.) of Material processed with TMP B	22
Figure 15.	Ductility (% Elong.) of Material processed with TMP C	23
Figure 16.	Ductility (% Elong.) of Material processed with TMP D	24
Figure 17.	Ductility (% Elong.) of Material processed with TMP E	25
Figure 18.	TMP B Strain rate sensitivity (m)	26
Figure 19.	TMP B Variation of strain rate sensitivity	27
Figure 20.	TMP B 'as rolled'	29
Figure 21.	TMP B grip section	30
Figure 22.	TMP B necked region	31
Figure 23.	TMP E grip section	31
Figure 24.	TMP E as rolled	32
Figure 25.	Stress Strain Curve for TMP A	36
Figure 26.	Stress Strain Curve for TMP A	37
Figure 27.	Stress Strain Curve for TMP A	38
Figure 28.	Stress Strain Curve for TMP B	39
Figure 29.	Stress Strain Curve for TMP B	40
Figure 30.	Stress Strain Curve for TMP B	41
Figure 31.	Stress Strain Curve for TMP C	42

Figure 32. Stress Strain Curve for TMP C	43
Figure 33. Stress Strain Curve for TMP C	44
Figure 34. Stress Strain Curve for TMP D	45
Figure 35. Stress Strain Curve for TMP D	46
Figure 36. Stress Strain Curve for TMP D	47
Figure 37. Stress Strain Curve for TMP E	48
Figure 38. Stress Strain Curve for TMP E	49
Figure 39. Stress Strain Curve for TMP E	50
Figure 40. TMP A Strain rate sensitivity (m)	51
Figure 41. TMP C Strain rate sensitivity (m)	52
Figure 42. TMP D Strain rate sensitivity (m)	53
Figure 43. TMP E Strain rate sensitivity (m)	54
Figure 44. TMP A Variation of strain rate sensitivity	55
Figure 45. TMP C Variation of strain rate sensitivity	56
Figure 46. TMP D Variation of strain rate sensitivity	57
Figure 47. TMP E Variation of strain rate sensitivity	58

ACKNOWLEDGEMENTS

I would like to express my gratitude to Professor Terry McNelley for providing insight and direction in this research endeavor. I wish to thank Mr. Tom Kellogg, Mr. Rob Hafley and Mr. Tom McCord for their technical support. A special thank-you goes to my wife, Ruth, for her patience, understanding and encouragement during my studies at the Naval Postgraduate School.

I. INTRODUCTION

Small modifications to processing and to alloy composition may have drastic effects on various mechanical properties of the resultant material. Metallurgists continuously explore the reasons for such changes in behavior, and exploit these properties to meet the demands of today's science and industry.

The aerospace industry has always been on the forefront of technology. One basic aspect of this field which has been of utmost concern since the days of (and prior to) Orville and Wilbur Wright, is how to get more payload in the air. Aluminum alloys are the predominant materials of airframe construction because of their high strength-to-weight ratio when used as beam structures and aircraft skin. Criteria used to evaluate metals for aerospace applications begin with relative strength and density. Other important criteria include resistance to cyclic fatigue, corrosion resistance, weldability and appearance. Many materials have adequately met these criteria and are in wide use today. Factors which spur continued research in high strength Aluminum alloys are cost of raw material production, fabrication and life-cycle costs.

The Naval Postgraduate School in combined efforts with the Naval Air Development Center is investigating an Aluminum-Magnesium-Lithium alloy, NAVALITE, to determine its potential applications as a high strength, low density alloy which may be fabricated by a means of superplastic deformation. Superplastic forming involves the deformation of a flat sheet of metal into a mold containing deep beads and sharp radii producing a monolithic structure. The benefits of molding as opposed to machining are obvious, and the ability to form a one-piece structure as opposed to an assemblage of machined parts and fasteners has a variety of payoffs. Overall strength-to-weight is increased due to fewer fasteners and co-located stress-risers. Corrosion resistance is improved due to fewer seams and joints. Fabrication costs are dramatically improved due to the relative ease and speed of superplastically forming a part.

As evidence, a nacelle center beam frame on the B-1 Bomber was redesigned and fabricated by Rockwell International Corporation to demonstrate the merit of superplastic forming. One component comprising the assemblage of eight parts and 96 fasteners was replaced with one superplastically formed part. Cost and weight studies concluded a 30% weight savings and more than 50% cost savings for the superplastic formed part.[Ref. 1]

Superplastic Aluminum alloys are not new. However, all superplastic alloys have drawbacks which in some way limit their usefulness. These limitations include only moderate tensile strengths and possible cavitation during forming due to high forming temperatures ($>500^{\circ}\text{C}$). Current research at the Naval Postgraduate School is pursuing improvement in mechanical properties as well as reducing the required high deformation temperatures. Such improvements are believed achievable through proper alloy composition and subsequent thermomechanical processing. This initial investigation into NAVALITE, with a view towards maximizing superplastic deformation, will attempt to determine an optimum thermomechanical process (TMP).

II. BACKGROUND

A. ALLOYS OF ALUMINUM

1. Al-Mg

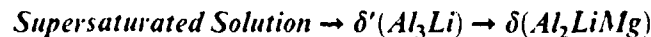
Aluminum-Magnesium represent nearly half the Aluminum production by tonnage. Low Mg alloys (<4 wt. pct. Mg) are characterized by good weldability, ductility, forming characteristics, and corrosion resistance. Low Mg alloys are of moderate strength. Intermediate Magnesium content, Al-Mg alloys (up to ≈ 7 wt. pct. Mg) exhibit the same qualities of a low Al-Mg alloy, however, become more difficult to cast.

High Al-Mg (≈ 10 wt. pct. Mg) are characterized by high strength, with good ductility and impact resistance. These alloys are vulnerable to inter-granular corrosion due to the β -phase precipitate. It is a misconception that β -phase precipitation is a strengthening mechanism. The β -phase is an incoherent precipitate which prefers grain boundaries, as opposed to forming a fine, uniformly dispersed precipitate which would impart strengthening via dislocation bowing. The strengthening mechanism in high Al-Mg alloy is solid solution strengthening. After conventional heat treatment, elevated ambient temperature conditions will result in reduced tensile strength and increased susceptibility to inter-granular corrosion. At slightly higher temperatures, self aging may result in loss of ductility and impact resistance. [Ref. 2: p. 338]

2. Al-Mg-Li

As an addition to Al-Mg alloys, Lithium offers a significant decrease in density and increase in modulus of elasticity. Lithium has a high solubility in Aluminum (5.2%) in the binary Al-Li system. Greatly improved strengths result due to the δ' (Al_3Li phase) precipitation during age hardening [Ref. 2: p. 51]. For each percent Lithium addition, a 3.5% reduction in density is achieved.

Al-Mg-Li with less than 1.5% Lithium acts as a quasi-binary Al-Mg alloy. For Lithium additions greater than 1.5% the Al-Li-Mg alloys become ternary in nature (Figure 1) [Ref. 3: p. 555]. The precipitation sequence is:



The metastable precipitate, δ' , forms at low temperatures. The thermomechanical processing of this research requires a precipitate phase to act as a stabilizing agent. The δ' is thought to be too small to interact with sub boundaries

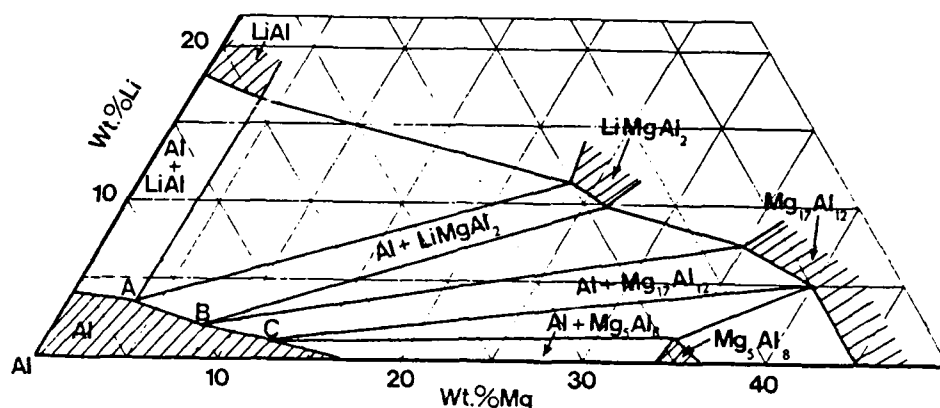


Figure 1. Aluminum Corner of the Al-Mg-Li Phase Diagram at 460°C

consisting of dislocations formed during TMP. Upon aging, δ' converts to δ . The δ -phase is of a size similar to that of β in the Al-Mg system and is anticipated to act as a stabilizing agent for substructures evolving during TMP. The effectiveness of δ is believed to be a function of its size and this depends in turn on heat treatment and the details of TMP.

Two strengthening mechanisms occur in Al-Mg-Li systems containing 1.5-2.5 wt. pct. Li, 4-7 wt. pct. Mg. When aged at low temperature (120-170°C) for approximately 12 hours, δ' , a phase of spheroidal shape strengthens by age hardening. The δ' (Al_3Li) is believed to be responsible for the good mechanical properties in the Al-Mg-Li system. The Magnesium which replaces Lithium in solid solution also contributes to strength. It should be noted that after superplastic forming the deformed component can be solution treated once again and aged to precipitate δ' .

Conversion at high temperatures of the metastable δ' (Al_3Li) to δ (Al_2LiMg) offers very little strengthening improvement. In the quasi-binary Al-Li system, Mg, here again, contributes as a solid solution strengthening mechanism. [Ref. 4: p. 115]

3. NAVALITE

NAVALITE, composition Al-2.70Mg-2.00Li-0.50Cu-0.13Zr (wt.pct.) falls in the quasi-binary region of Al - Al_2LiMg . This alloy exhibits 60-65 ksi yield strength, 8% elongation and good notch toughness in a T6 condition as reported by Lee [Ref. 5]. The high Lithium content produces a low density alloy of about 2.5 g cc

[Ref. 3: p. 555]. This compares with Al-7075 at a density of 2.8 g/cc [Ref. 6]. This confers a high strength-to-weight ratio.

B. CONDITIONS FOR SUPERPLASTICITY

1. Grain Size

It is generally recognized that grain refinement is essential to superplasticity. Typically, values of grain size of less than 10 μm are required to support a superplastic response. An optimum size of 1 to 2 μm is desired to facilitate forming at reduced temperature and thus diminish cavitation during superplastic forming.

2. Second Phase

Grain refinement is most easily accomplished in a two phase structure. A precipitate enhances grain refinement when it is present in large quantity, is of fine size itself and uniformly distributed throughout the matrix [Ref. 7: p. 367]. One method to achieve grain refinement is by continuous recrystallization of the alloy during warm rolling, such that precipitation of a fine, intermetallic compound is produced concurrently with a highly refined subgrain structure. The precipitate acts as a stabilizing agent, pinning the subgrain structure to the precipitate. The precipitate prevents complete recrystallization by holding the recovered subgrain structure in a metastable state. By warm rolling, a size of 2.0 to 5.0 μm can be obtained. [Ref. 8]

3. Grain Boundary Sliding

A subgrain boundary typically is thought to have misorientations of 0.1 to 1.0 degree. It has been proposed that during the cyclic warm rolling and annealing process of this research, recovery will progressively increase the angle of misorientation of such low angle boundaries [Ref. 9: p. 1237]. High misorientation of sub boundaries, of the order of 2.0 to 7.0 degrees, apparently permits sufficient grain boundary sliding and grain rotation to occur during superplastic deformation. Deformation by sliding of grains along their mutual boundaries is frequently proposed to be the essential step in superplastic deformation. It is usually assumed that such sliding requires high-angle grain boundaries and that subgrain boundaries are insufficient for this purpose. Subgrain boundaries are composed of dislocation arrays and in between such dislocations the lattice is in high registry across the boundary and thus sliding is inhibited. Grain rotation is also accommodated by the structure when some of the grains within the structure are allowed to slip. [Ref. 10]

4. Strain Rate Sensitivity and Phenomenological Aspects

The phenomenon of superplastic deformation is the ability to deform in excess of 200% while inhibiting the formation of localized "necks". It has been observed that all superplastic materials have a property in common, that is a strong relationship of flow stress to strain rate in the power law relationship:

$$\sigma = K\dot{\epsilon}^m$$

The higher the m-value in this equation, i.e., as m approaches 1.0, the greater the potential superplastic response. Generally, m is referred to as the strain rate sensitivity coefficient [Ref. 9: p. 1229]. Highly superplastic metals with ductilities in the range of 1000% will have an m value of 0.5 or higher.

The value of m for an alloy can be found from experimental data by determining the slopes on double logarithmic coordinates according to:

$$m = \frac{\partial \ln \sigma}{\partial \ln \dot{\epsilon}}$$

The strain rate of maximum elongation can be experimentally predicted by the value of m. Although it is observed that superplastic metals have values of $m \sim 0.5$, it should be noted that this is not a sufficient condition for superplasticity.[Ref. 7: p. 364]

5. Thermomechanical Processing

Thermomechanical processing (TMP) is intended to develop a fine grained microstructure (1 - 2 μm) capable of grain boundary sliding. TMP in this research is initiated by homogenizing the cast metal in the solid state. This is accomplished at a temperature above T_{solvus} by heating for a period of about 24 hours. A series of warm rolls and recovery periods then produces the fine grained microstructure capable of superplastic deformation (SPDF).

Warm rolling, defined as rolling at temperatures greater than 200°C, but below the recrystallization temperature, will create a high dislocation density in the deformed metal. This is followed by recovery in an annealing oven. A fine, subgrain structure is formed as fine precipitates come out of solution and interact with the dislocation network. This process of static, continuous recrystallization may be thought of as the nucleation process preceding boundary migration in discontinuous recrystallization. That is, the subgrain structures impinge before growth of the grain can occur. Continuous recrystallization is characterized by progressive grain refinement to the size of 1 - 2 μm and an increase in misorientation of low-angle grain boundaries into higher angle

grain boundaries. A refined microstructure and sufficiently high angle boundaries, again, are prerequisite to superplastic forming. [Ref. 7: p. 369]

Superplasticity in Al-Mg alloys was achieved by McNelley et.al. by warm rolling and annealing of previously solution treated billets to a true strain of 2.5 at a temperature of 300°C (Figure 2). This was attributed to continuous recrystallization during isothermal rolling [Ref. 11]. A cycle of reductions of ten percent (of original thickness) per pass by warm rolling at 300°C with each pass followed by a 30 minute anneal at 300°C produced high-Mg Aluminum alloys capable of superplastic deformation. This TMP represents the initial process in this study on NAVALITE.

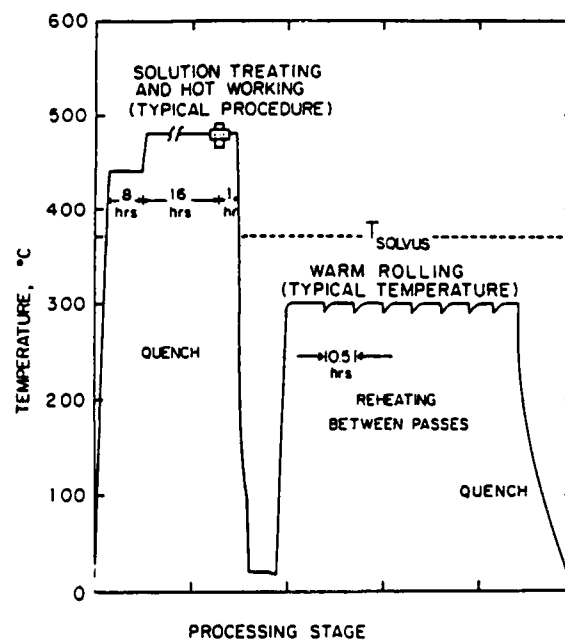


Figure 2. TMP Employed on Al-10Mg, Al-10Mg-1Li

III. EXPERIMENTAL PROCEDURE

A. CASTING AND SECTIONING

NAVALITE casting number 606170A, of composition Al-2.7Mg-2.04Li-0.5Cu-0.13Zr and with impurities not exceeding 0.05Fe-0.04Se-0.018Ti (wt.pct.) was received in cast form with dimensions 6.0in x 3.5in x 2.5in (152.4mm x 88.9mm x 63.5mm). The casting was sectioned into ten billets for subsequent solution treatment and processing. The billet dimensions were 3.5in x 1.25in x 1.25in (88.9mm x 31.8mm x 63.5mm). Scrap material was sectioned into coupons for an initial solution treatment study.

B. SOLUTION TREATMENT STUDY

A solution treatment time-temperature study was conducted to determine a sufficient homogenization treatment (Table 1). Optical microscopy was conducted on "as cast" sample coupons, solution treatment test coupons and samples from subsequently forged billets utilizing a Zeiss ICM-405 optical microscope.

Table 1. SOLUTION TREATMENT STUDY

TEST	SOLUTION TREATMENT
1	8 hours @ 400°C + 16 hours @ 535°C
2	8 hours @ 425°C + 16 hours @ 535°C
3	8 hours @ 450°C + 16 hours @ 535°C
4	8 hours @ 475°C + 16 hours @ 535°C
5	18 hours @ 475°C

C. THERMOMECHANICAL PROCESSING

Solution treatment of 4 hours at 450°C, followed by 16 hours at 535°C was selected. Two Lindberg type B-6 Heavy Duty furnaces were used for homogenization. Upset forging the billet at 450°C was performed in a Baldwin-Tate-Emery testing machine equipped with heated platens. Forging along the longitudinal axis of the billet resulted in a 3.5:1 reduction with a final thickness of approximately one inch. Forged billets were replaced in the 535°C furnace for one hour and subsequently quenched in water. A considerable amount of oxide was produced on the surface of the billet during solution

treatment. The forged billet was machined to a smooth surface by a series of fly cuts removing ≈ 0.031 inch (0.79mm) on the top and bottom faces and squaring the sides to reduce adverse rolling affects.

A logic chart was utilized to attempt to determine the optimum rolling scheme (Figure 3). Thermomechanical processing (TMP) was performed as listed in Table 2. Rolling schedules were varied to provide a means of changing the dislocation density imparted to the billet.

The forged billet was placed in a Blue M furnace, model 8655F-3, for 30 minutes at 300°C prior to each rolling reduction. A massive steel plate was located on the floor of the furnace to act as a heat capacitor in order to maintain a stable annealing temperature.

TMP, being the critical stage in producing a fine grained microstructure capable of superplastic deformation, was varied in five graduated processes designed to investigate the role of deformation temperature in increasing dislocation density. TMP A, TMP B and TMP E are schematically represented in Figures 4, 5 and 6, respectively.

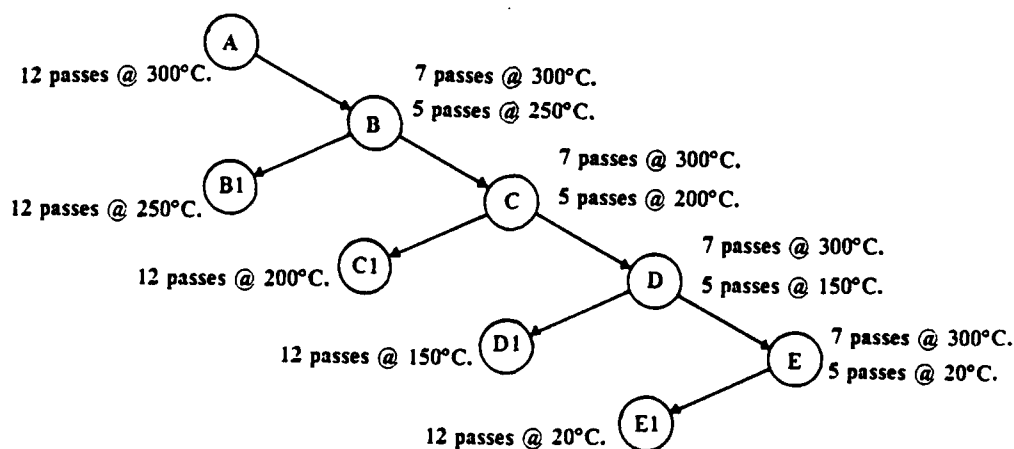


Figure 3. TMP Logic Chart

TMP B-E utilized a separate furnace to step down the temperature prior to each rolling pass. The samples were placed in a furnace at the reduced temperature for five minutes, again on top of a massive steel plate to quickly equilibrate prior to rolling. After each rolling pass, the sample was returned to the 300°C annealing furnace for 30 minutes. For the 20°C and the 150°C roll, care was taken to commence the 30 minute

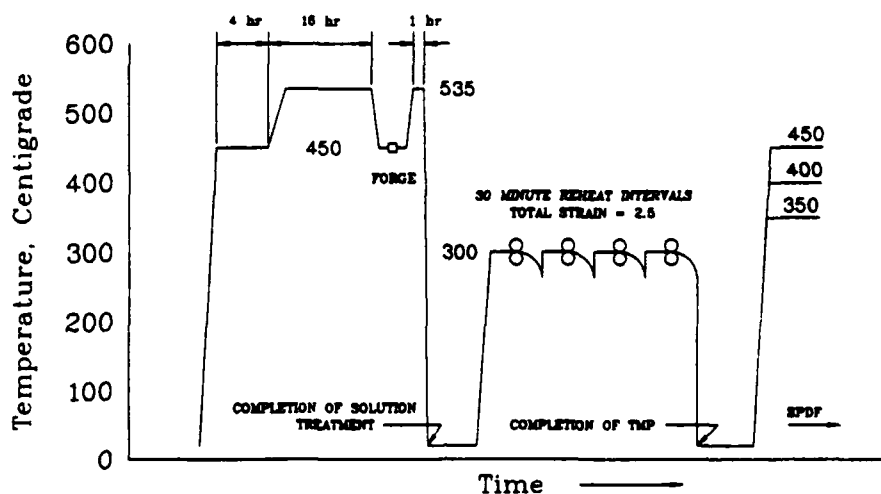


Figure 4. TMP for Sample A

Table 2. THERMAL MECHANICAL PROCESSING REGIMES

TMP	FIG.	SOLN TRTMT	FORGE TEMP	ROLLING TEMP	ANNEALING TEMP. TIME
A	4	450°C/535°C	450°C	12 passes @ 300°C	300°C @ 30 min
B	5	450°C/535°C	450°C	7 passes @ 300°C 5 passes @ 250°C	300°C @ 30 min
C		450°C/535°C	450°C	7 passes @ 300°C 5 passes @ 200°C	300°C @ 30 min
D		450°C/535°C	450°C	7 passes @ 300°C 5 passes @ 150°C	300°C @ 30 min
E	6	450°C/535°C	450°C	7 passes @ 300°C 5 passes @ 20°C	300°C @ 30 min

anneal "clock" once the temperature of the billet was above $\approx 265^{\circ}\text{C}$. The last rolling pass was followed by water quenching to room temperature.

Billets were rolled in a Fenn Laboratory Rolling Mill using the reduction scheme shown in Table 3. Ten percent (of original thickness) reductions for the first seven passes and 20 to 25% (of last pass thickness) reductions were utilized for the remaining five passes.

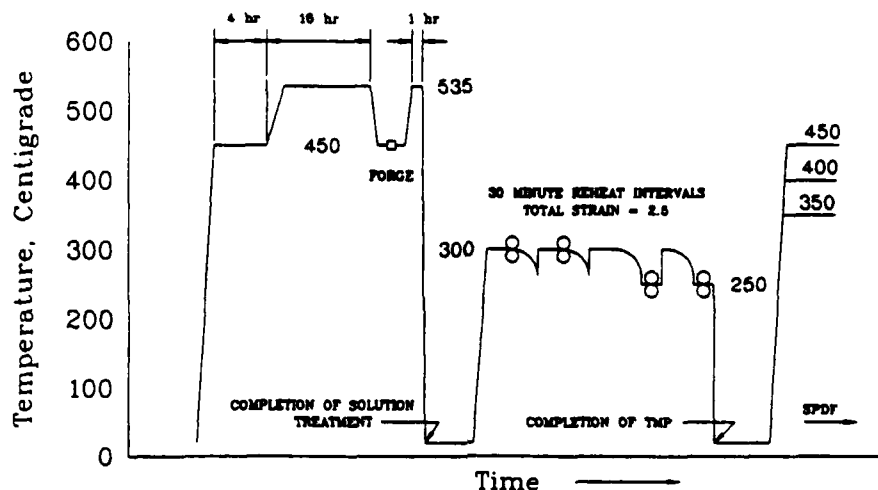


Figure 5. TMP for sample B

The resulting rolled strip, nominally 2 mm in thickness, was machined to dimensions for tensile testing (Figure 7). Occasionally, due to edge cracking, only limited quantities of tensile testing samples could be machined from the strip.

D. TENSILE TESTING

Tensile testing was performed on an Instron Model TT-D floor model Universal Testing Machine. Tensile testing temperature was maintained by a Marshall clamshell furnace model 2232. Samples were placed in preheated grips and the assembly was quickly placed within the clamshell and allowed to equilibrate to testing temperature for 30 minutes. Tension testing was conducted at 350°C to 450°C for the nominal strain rates of $6.67 \times 10^{-2} \text{ s}^{-1}$ to $6.67 \times 10^{-5} \text{ s}^{-1}$.

E. DATA REDUCTION

True stress vs. true strain curves were reduced from Instron chart data recorded as a function of load vs. time. The data were compensated for constant crosshead speed, such that stress vs. strain rate data is comparable. This correction is outlined by McNelley [Ref. 12].

Stress at a strain of $\epsilon = 0.1$ versus strain rate sensitivity data were plotted on double logarithmic coordinates for each test temperature to facilitate determination of the strain rate sensitivity coefficient m ($m = \partial \ln \sigma / \partial \ln \dot{\epsilon}$). The stress-strain data was similarly analyzed at other strains to assess the evolution of m with strain.

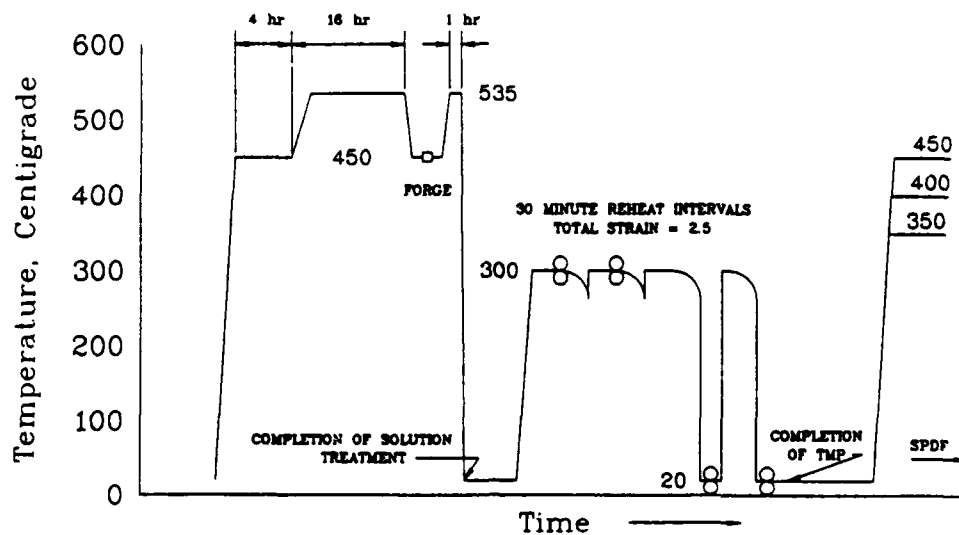


Figure 6. TMP for sample E

Table 3. ROLLING SCHEDULE

ROLL #	ROLL CHANGE (.08 in + .01 in)	MILL SETTING (right/left)	MILL GAP (in)	% STRAIN (per pass - relative to entering strain)
open	+(12 + 4)	0 0	.94	--
1	-(2 + 0)	0 0	.84	10.4
2	-(1 + 2)	6 6	.74	12.0
3	-(1 + 2)	4 4	.64	13.5
4	-(1 + 2)	2 2	.54	15.6
5	-(1 + 2)	0 0	.44	18.5
6	-(1 + 2)	6 6	.34	22.7
7	-(1 + 2)	4 4	.24	29.4
8	-(0 + 6)	6 6	.18	25.0
9	-(0 + 5)	1 1	.13	27.7
10	-(0 + 4)	5 5	.09	30.7
11	-(0 + 3)	2 2	.06	33.3
12	-(0 + 1.3)	0.7 0.7	.047	21.7

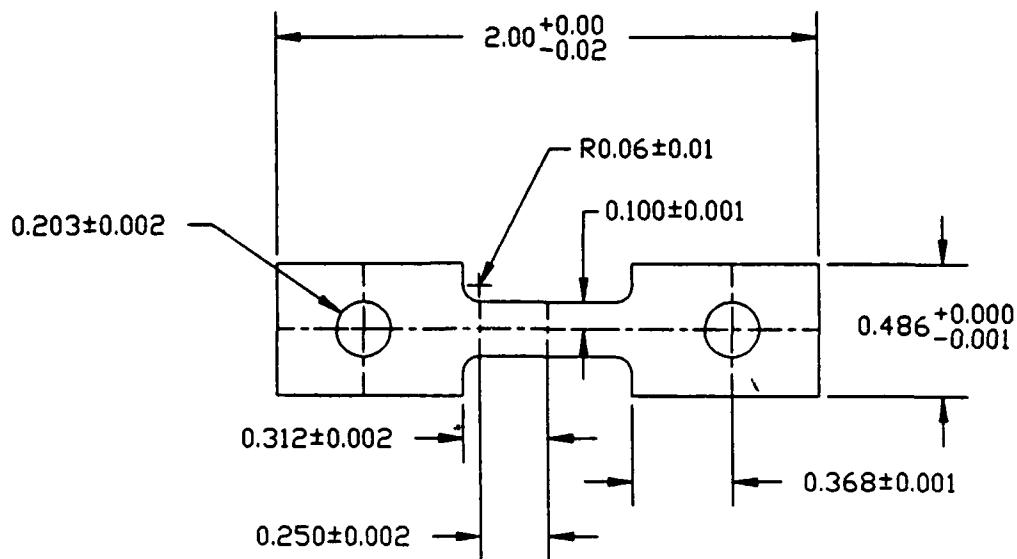


Figure 7. Tensile Test Specimen Drawing

F. OPTICAL MICROSCOPY

Optical microscopy was conducted in support of this research for assessment of the solution treatment study and of TMP comparisons. A Zeiss ICM-405 Optical Microscope was used. Sample specimens were mounted and polished using 6, 3, and 1 micron diamond paste and final polish with cerium oxide. Etching on cast samples utilized 40 seconds in Keller's solution plus 10 seconds in 0.4M nitric acid twice repeated. Etching of as rolled and deformed samples required 15 seconds in Keller's solution followed by 5 seconds in 0.4M nitric acid.

IV. RESULTS AND DISCUSSION

A. SOLUTION TREATMENT STUDY

The various solution treatments for homogenization of the cast material resulted in significant improvement in the microstructure. All appeared to provide adequate homogenization. Micrographs of the cast NAVALITE showed a large grain boundary eutectic. This is seen as large, black thick grain boundaries, the result of non-equilibrium solidification (Figure 8). This results in a grain boundary region of eutectic composition with a relatively low melting temperature and a cored grain interior which has a higher melting temperature.

Care must be taken not to initially homogenize higher than the eutectic temperature or microstructural porosity may result. An initial homogenization temperature was selected to be 450°C. Further homogenization can then be conducted at 535°C to bring the precipitates into solution.

Observation of the near fully homogenized NAVALITE showed that coring had disappeared. The eutectic at the grain boundary was significantly reduced. Few precipitates remain in the structure, although some porosity is apparent. The latter defect was of concern and could not be eliminated by reduced temperatures in the initial homogenization step. (Figure 9)

It was decided to proceed with solution treating and forging of an actual billet and look for further improvement in the grain structure resulting from mechanical working. Forging nearly eliminated all the voids which were produced during casting. The forged billet now appeared to be fully homogenized and ready for further TMP. (Figure 10)

B. ROLLING AT 300°C

The initial TMP schedule (TMP A) for NAVALITE was that determined to be optimal in study of Al-10wt.pct.Mg-0.1wt.pct.Zr and Al-8wt.pct.Mg-1.0wt.pct.Li-0.2 wt.pct alloys, which produced maximum ductilities of $\approx 600\%$ and $\approx 1100\%$, respectively [Ref. 13: p. 51]. Maximum elongation obtained with NAVALITE was 350% at 400°C at a strain-rate of $6.67 \times 10^{-4} \text{ s}^{-1}$ (Table 4).

Although NAVALITE ductility had considerably less superplastic response than the 10 wt.pct. Mg and 8wt.pct.Mg 1wt.pct.Li alloys, it is well above the nominal 200% criterion recognized as a threshold for superplasticity (see Table 4). It should be noted that when work on the high Mg and high Mg, low Li alloys had first begun, ductilities

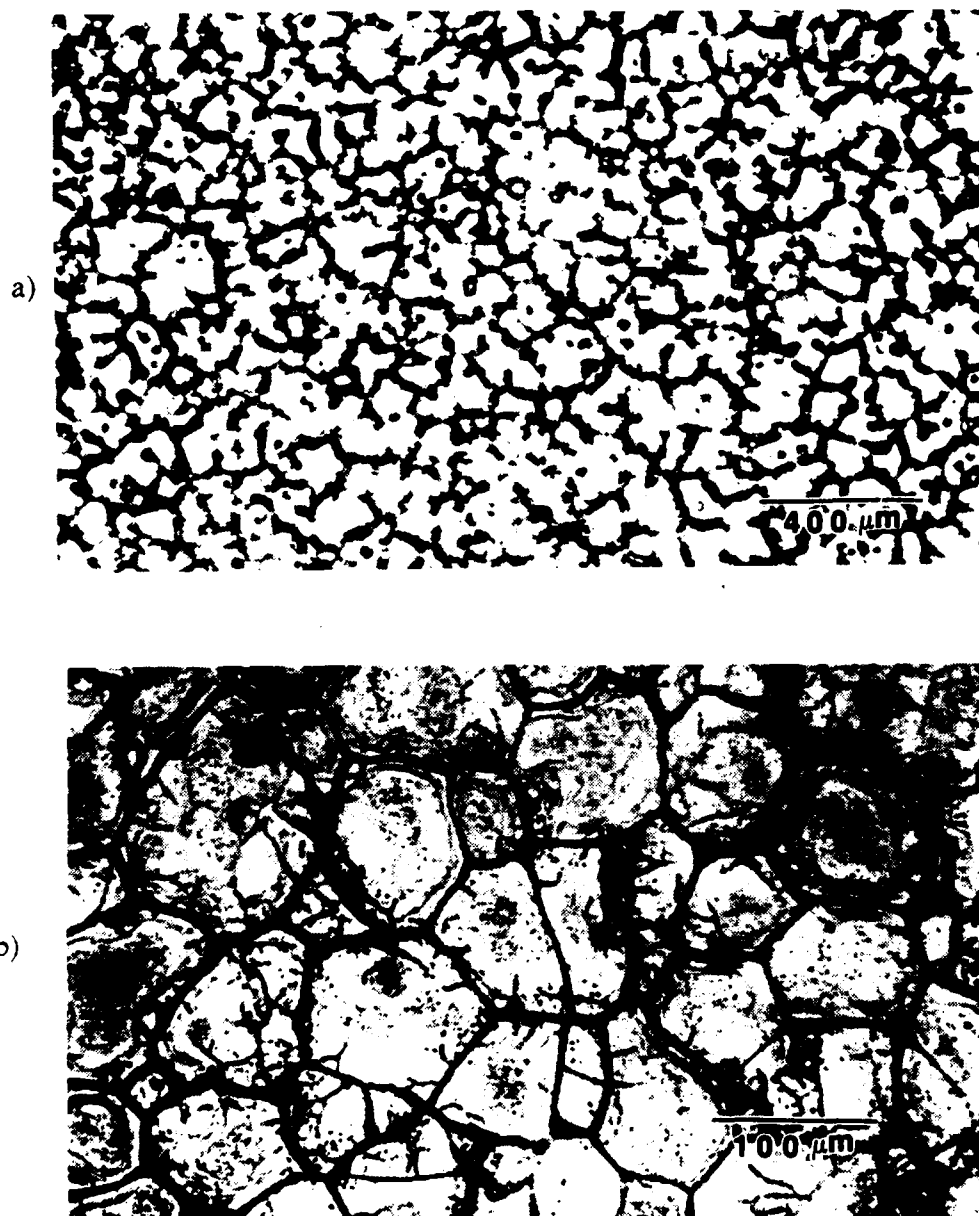
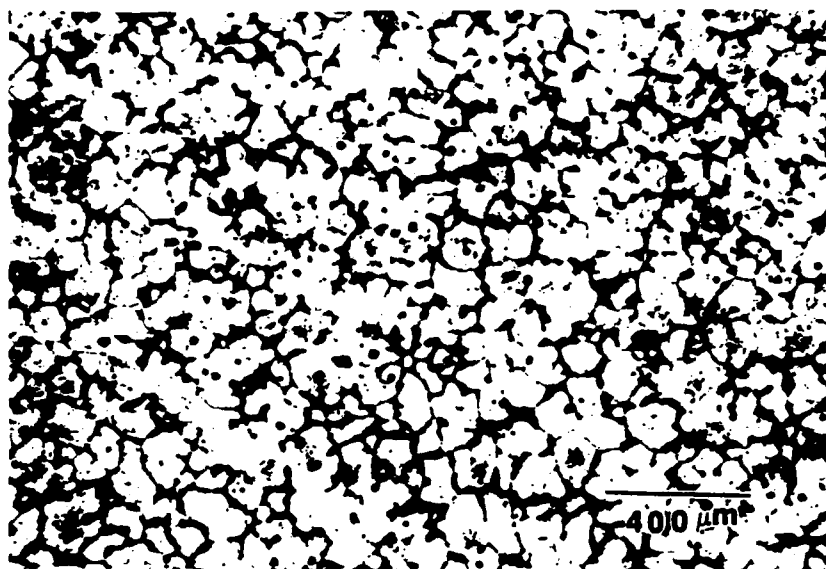


Figure 8. Cast NAVALITE billet #606170A(N2): a) Shows large amount of eutectic remaining at the grain boundary due to non-equilibrium cooling. (55X) b) Grains appear to be cored. (220X)

a)



b)

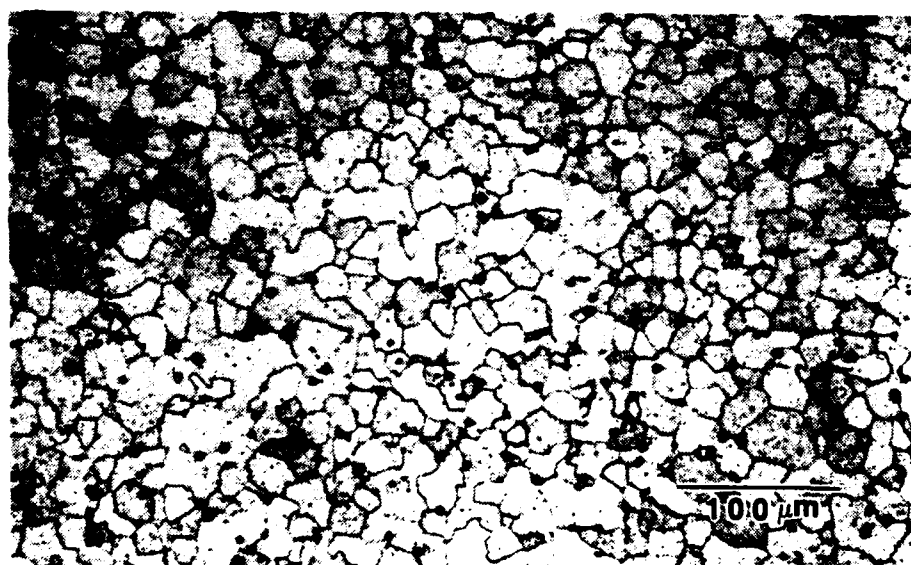


Figure 9. NAVALITE casting after solution treatment #3: a) 8 hours at 450°C and quench. (50X) b) 8 hours at 450°C followed by 16 hours at 535°C and quench. Small globules of eutectic remaining at the triple points. (55X)

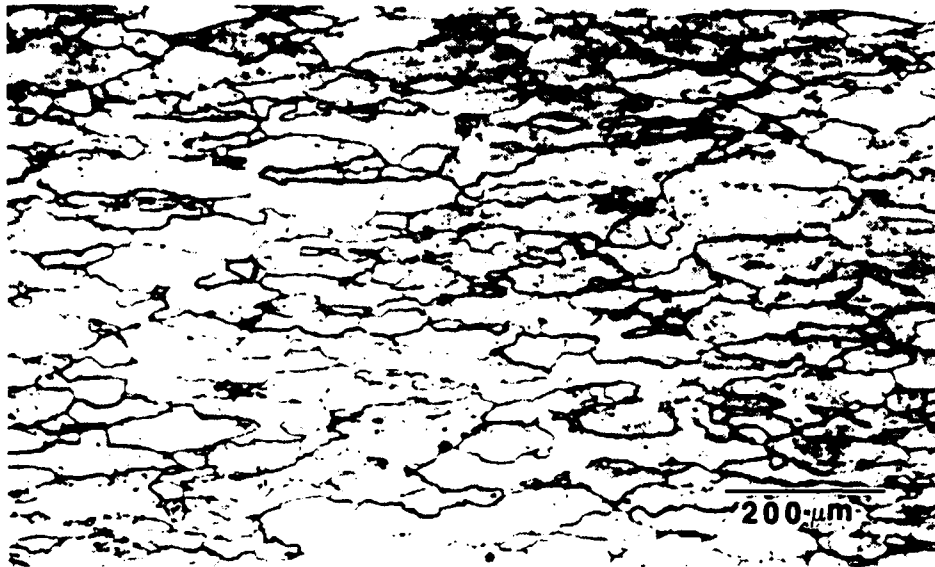


Figure 10. NAVALITE after solution treatment and forging: Grains are near fully homogenized after hot-working. (100X)

Table 4. DUCTILITY (% ELONG.) OF MATL. PROCESSED WITH TMP A

	350°C	400°C	450°C
$6.67 \times 10^{-2} \text{ s}^{-1}$	169	200	184
$6.67 \times 10^{-3} \text{ s}^{-1}$	181	306	240
$6.67 \times 10^{-4} \text{ s}^{-1}$	150	350	300
$6.67 \times 10^{-5} \text{ s}^{-1}$	---	244	---

reported were in the same 350% range as found on this first test of NAVALITE [Ref. 13: p. 51]. Monroe's work on Al-6.0 wt.pct.Mg-2.0 wt.pct.Li, the first testing of any Al-Mg-Li alloy of Lithium content greater than 1.5%, found that processing was impossible due to edge cracks while rolling. NAVALITE, of nominal 2.7 wt. pct. Mg and 2 wt. pct. Li, showed no signs of difficulty in rolling.

It is postulated that this lower Mg content and higher Li content has placed NAVALITE at a different operating point relative to the solvus temperatures for the phases present.

C. VARIATION IN TMP ROLLING TEMPERATURES

An investigation into the possibility of further improvements of ductility was pursued. Increasing dislocation density by rolling at lower temperatures was pursued as a means of attaining further grain refinement. Annealing temperature and time were held constant at 300°C and 30 minutes, respectively. Initial results from TMP B indicated rolling temperature may have important effects as a processing variable (Table 5).

Table 5. DUCTILITY (% ELONG.) OF MATL. PROCESSED WITH TMP B

	350°C	400°C	450°C
$6.67 \times 10^{-2} \text{ s}^{-1}$	150	203	178
$6.67 \times 10^{-3} \text{ s}^{-1}$	191	341	309
$6.67 \times 10^{-4} \text{ s}^{-1}$	231	428	341
$6.67 \times 10^{-5} \text{ s}^{-1}$	---	294	294

TMP B produced the highest ductility attained in this study of NAVALITE, 428%. A temperature of 250°C in the last five passes to impart a higher dislocation density, and again a test temperature of 400°C at a strain rate of $6.67 \times 10^{-4} \text{ s}^{-1}$, resulted in maximum elongation. The billet rolled easily with no adverse cracking (Figure 11, Figure 12).

As the rolling temperatures in processes C-E were reduced, edge cracking became a significant problem during the final rolling passes. Also, hairline surface cracks traversed the face of the billet but would not necessarily cause a complete fracture. TMP E (rolled at room temperature) resulted in a maximum ductility of 425%, however edge cracking was so severe that only a small portion of the final strip could be salvaged for tensile testing.

It should be noted that in each TMP schedule, maximum superplasticity was achieved using a test temperature of 400°C and strain rate of $6.67 \times 10^{-4} \text{ s}^{-1}$ (Figure 13, Figure 14, Figure 15, Figure 16, Figure 17). Also, the maximum elongation for all TMP schedules, accounting for experimental scatter, was of the order of 400%. For TMP B, as in all TMP's, calculated strain rate sensitivity (m) coefficient values were approximately equal to 0.3 at a strain of $\epsilon = 0.1$ (Figure 18), $m = 0.5$ being that of a highly superplastic material. Reducing rolling temperature below 250°C did not enhance ductilities.

Stress-strain curves, having been compensated for constant crosshead speed during testing, indicated microstructural coarsening to be occurring during straining and

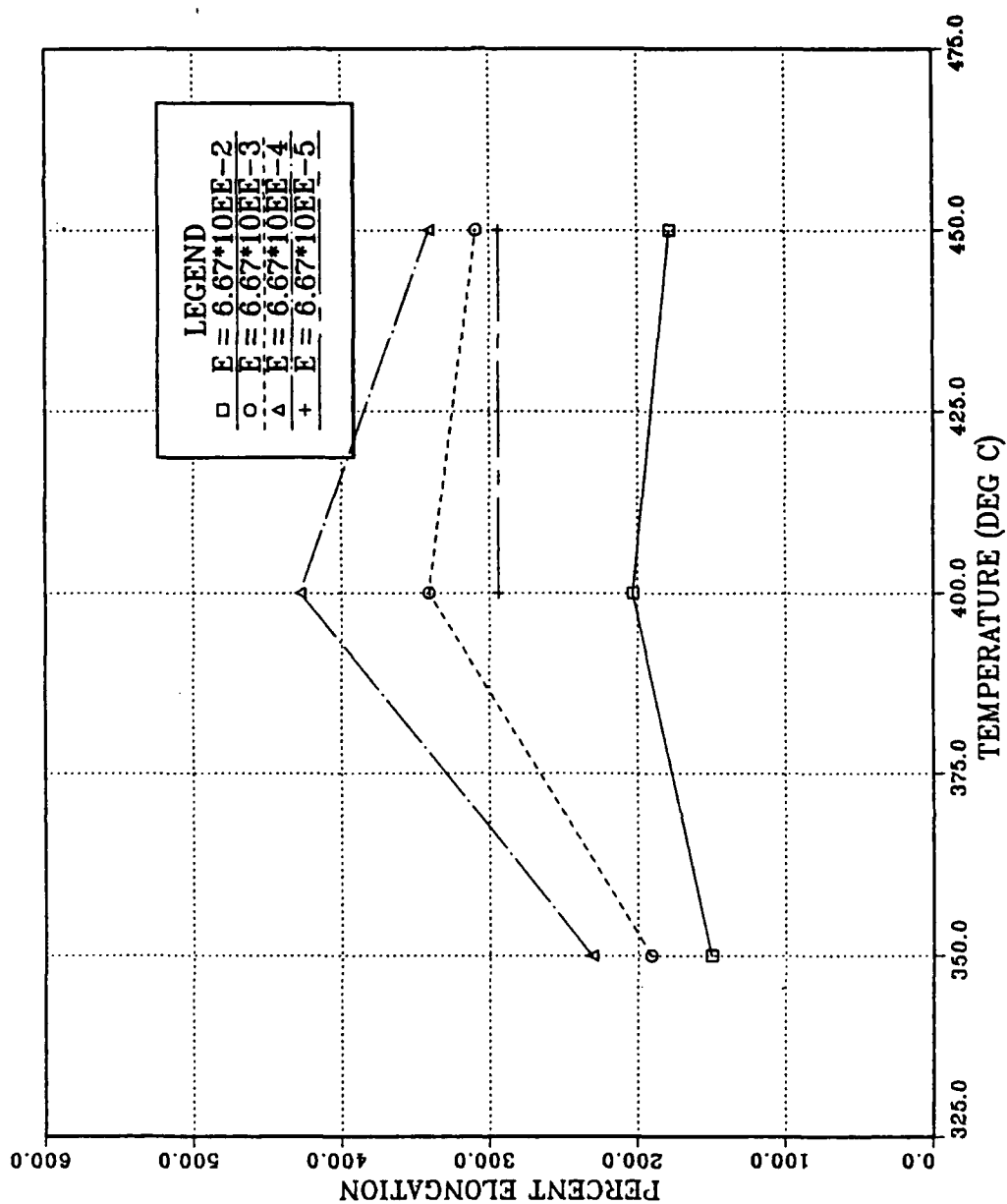


Figure 11. TMP B - Percent elongation vs. temperature: Maximum elongation of 428% occurs at 400°C, $\dot{\epsilon} = 6.67 \times 10^{-4} \text{ s}^{-1}$

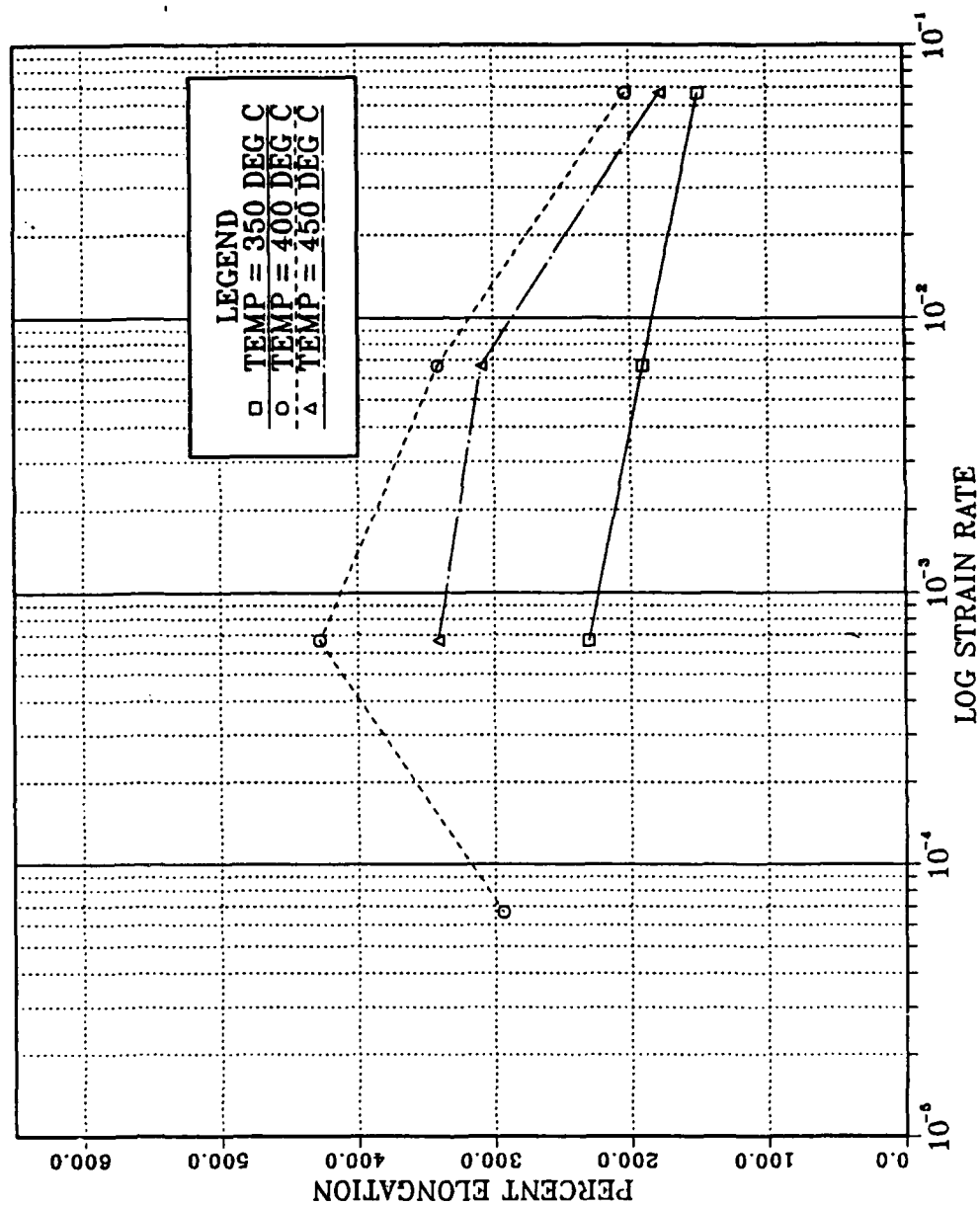


Figure 12. TMP B - Percent elongation vs. strain rate: Maximum elongation of 428% occurs at 400°C, $\dot{\epsilon} = 6.67 \times 10^{-4} \text{ s}^{-1}$

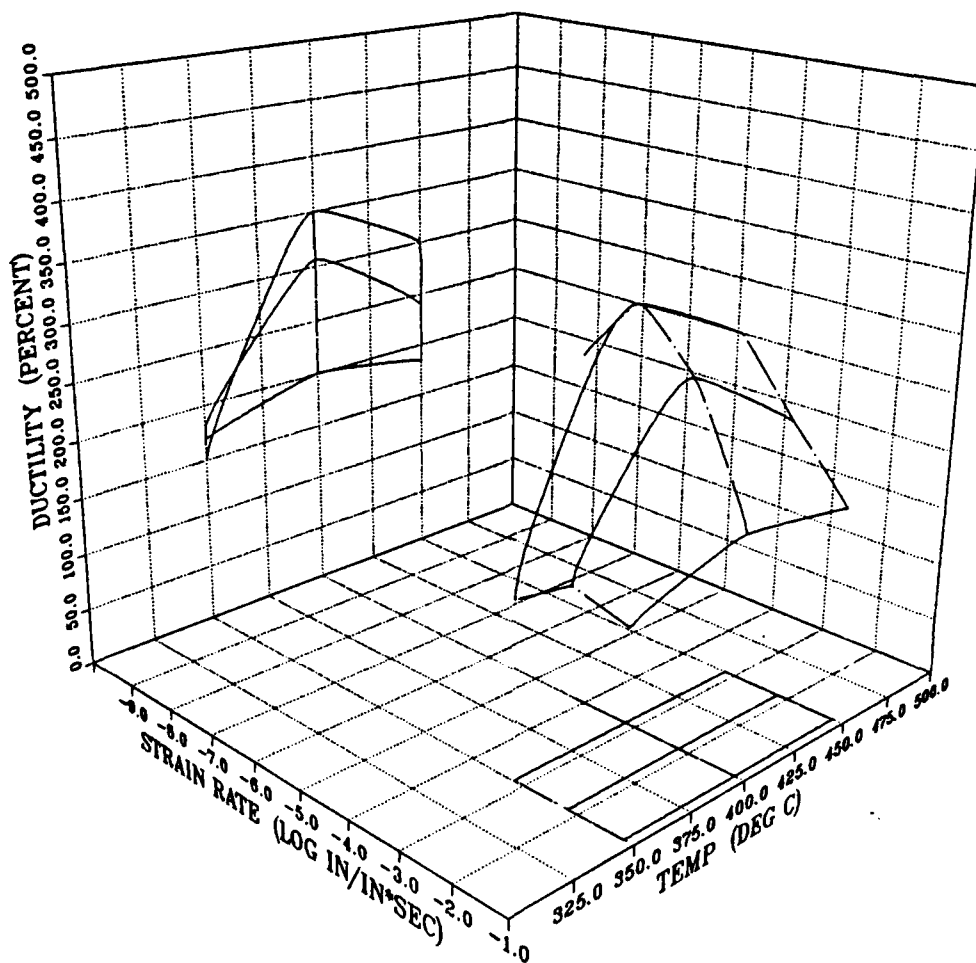


Figure 13. Ductility (% Elong.) of Material processed with TMP A: Maximum elongation of 350% occurs at $T = 400^{\circ}\text{C}$, $\dot{\epsilon} = 6.67 \times 10^{-4} \text{ s}^{-1}$

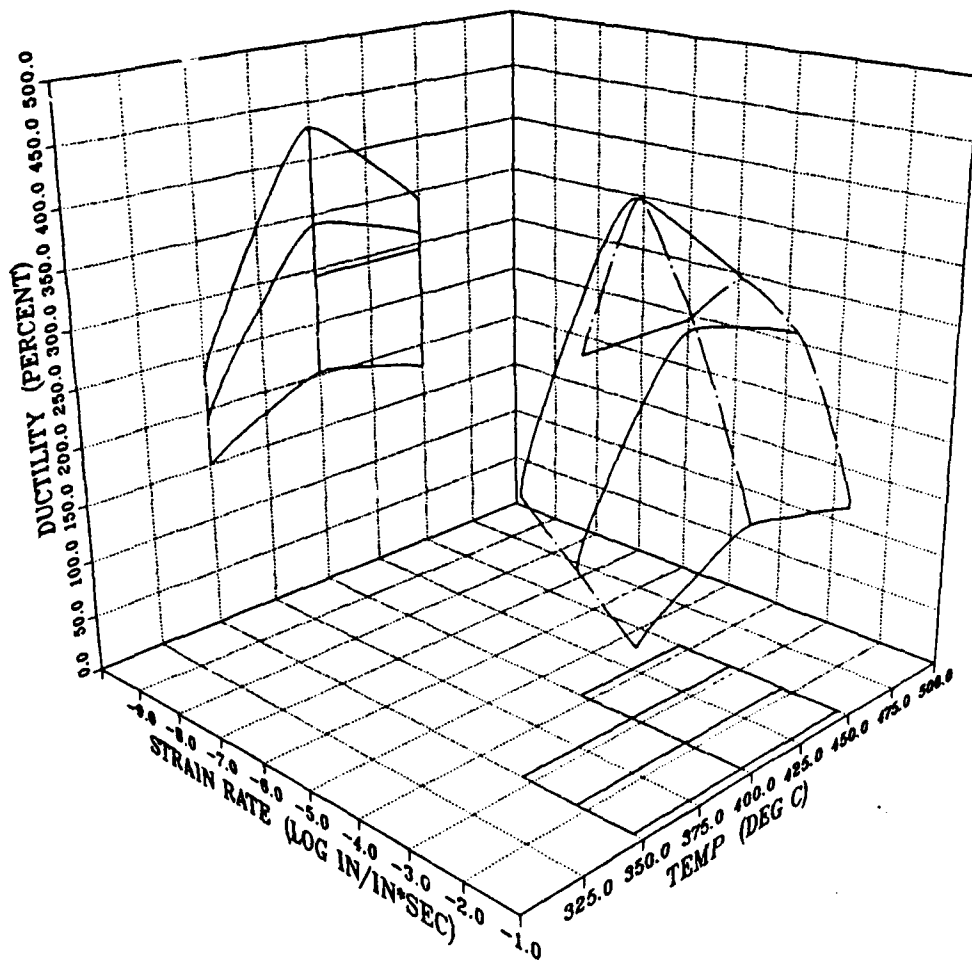


Figure 14. Ductility (% Elong.) of Material processed with TMP B: Maximum elongation of 428% occurs at $T = 400^{\circ}\text{C}$, $\dot{\epsilon} = 6.67 \times 10^{-4} \text{ s}^{-1}$

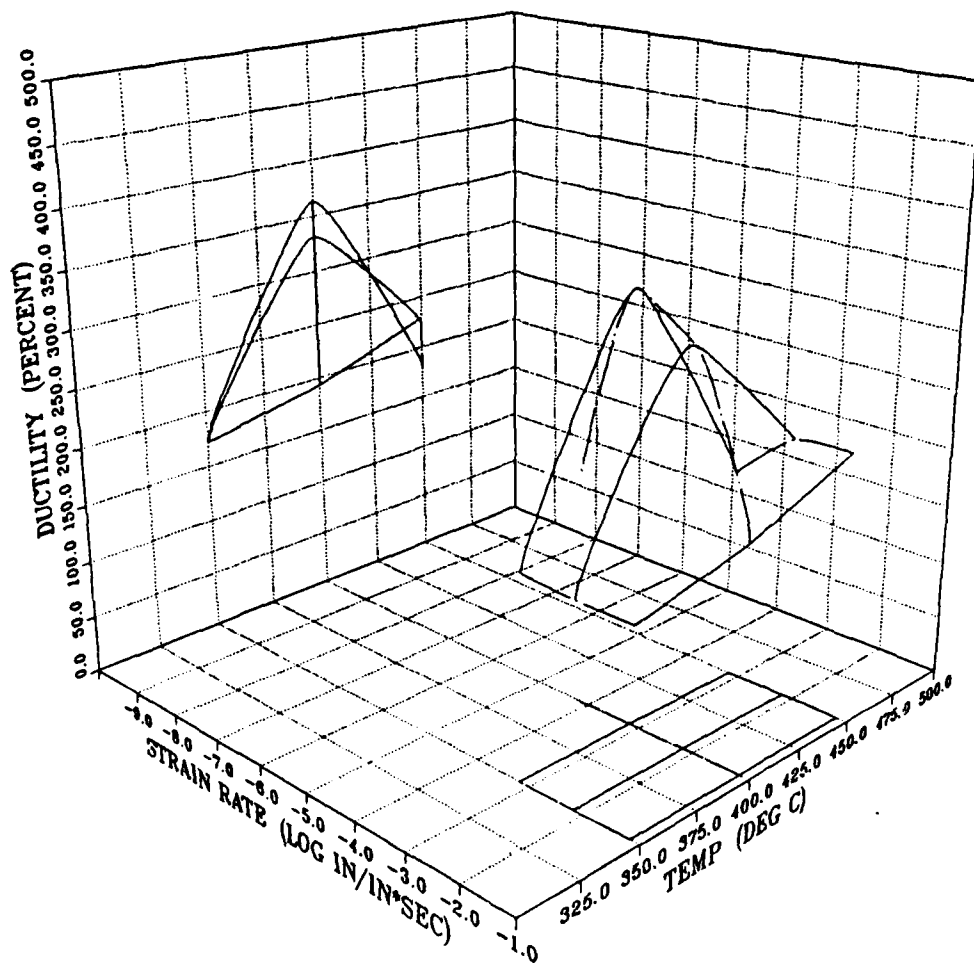


Figure 15. Ductility (% Elong.) of Material processed with TMP C: Maximum elongation of 363% occurs at $T = 400^{\circ}\text{C}$, $\dot{\epsilon} = 6.67 \times 10^{-4} \text{ s}^{-1}$

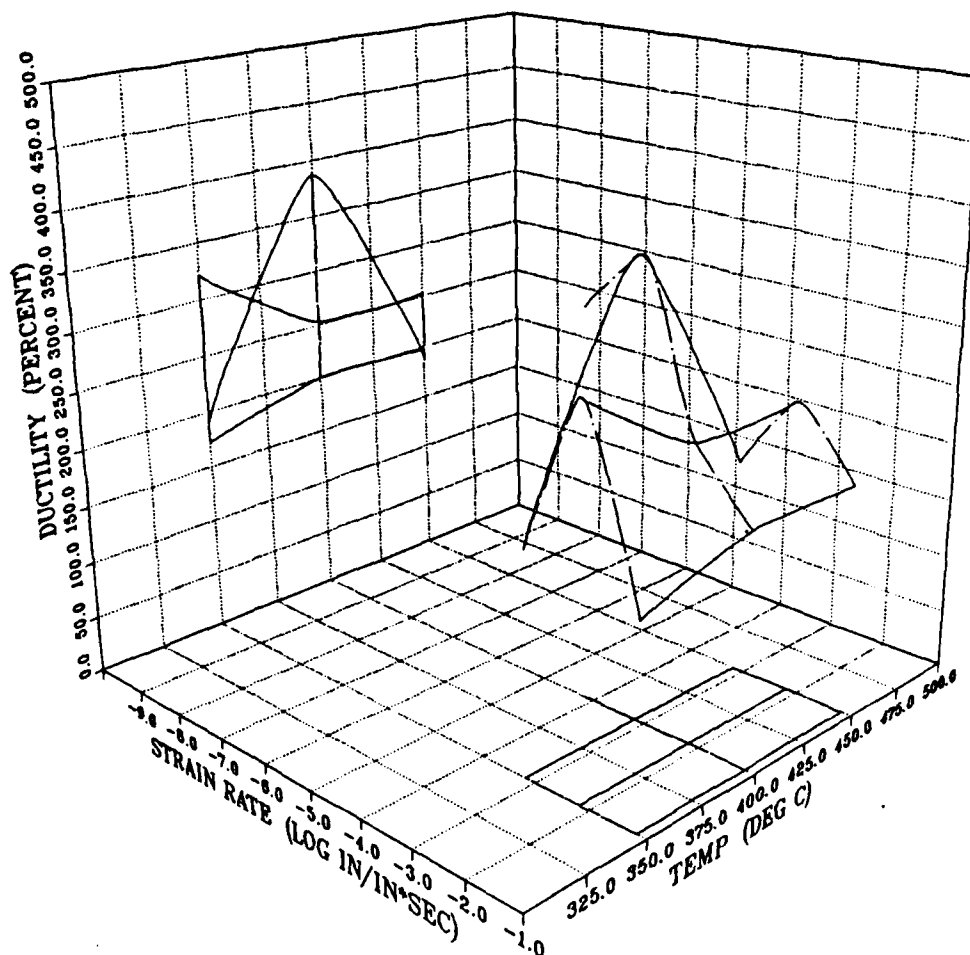


Figure 16. Ductility (% Elong.) of Material processed with TMP D: Maximum elongation of 387% occurs at $T = 400^{\circ}\text{C}$, $\dot{\epsilon} = 6.67 \times 10^{-4} \text{ s}^{-1}$

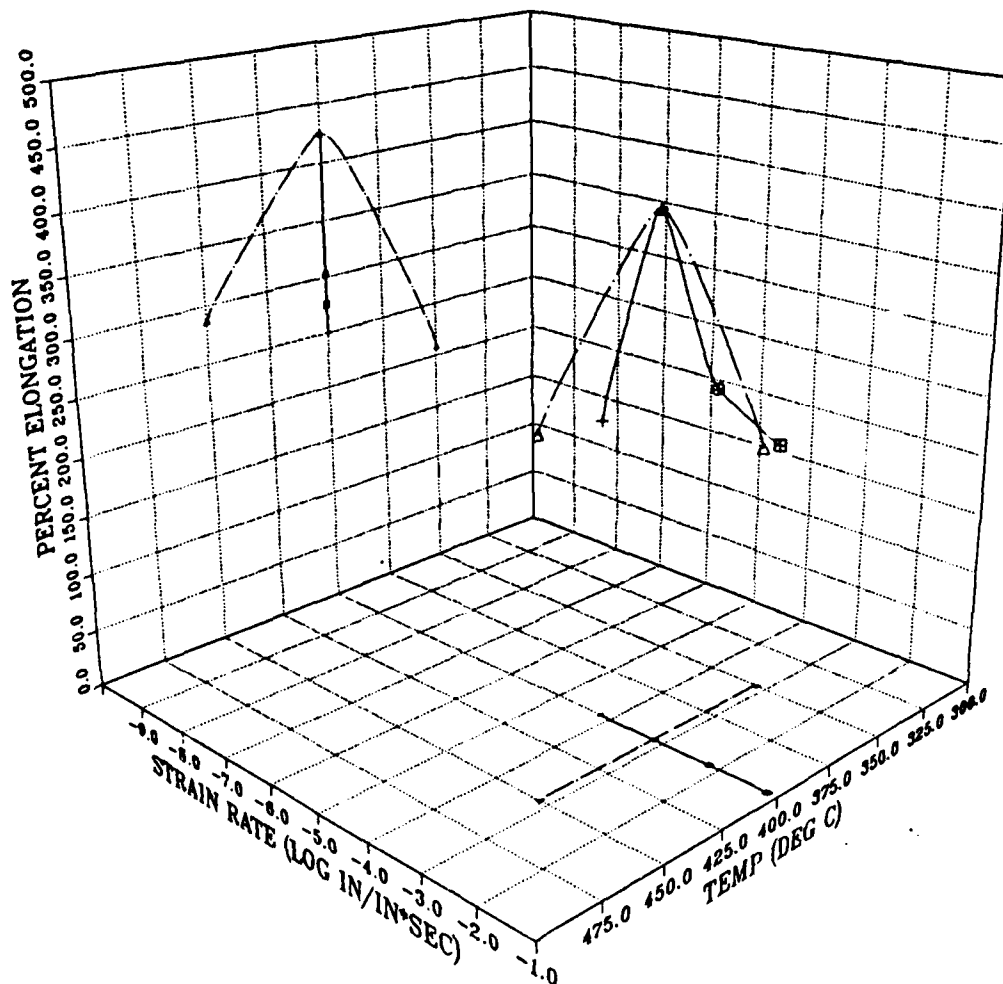


Figure 17. Ductility (% Elong.) of Material processed with TMP E: Maximum elongation of 425% occurs at $T = 400^{\circ}\text{C}$, $\dot{\epsilon} = 6.67 \times 10^{-4} \text{ s}^{-1}$

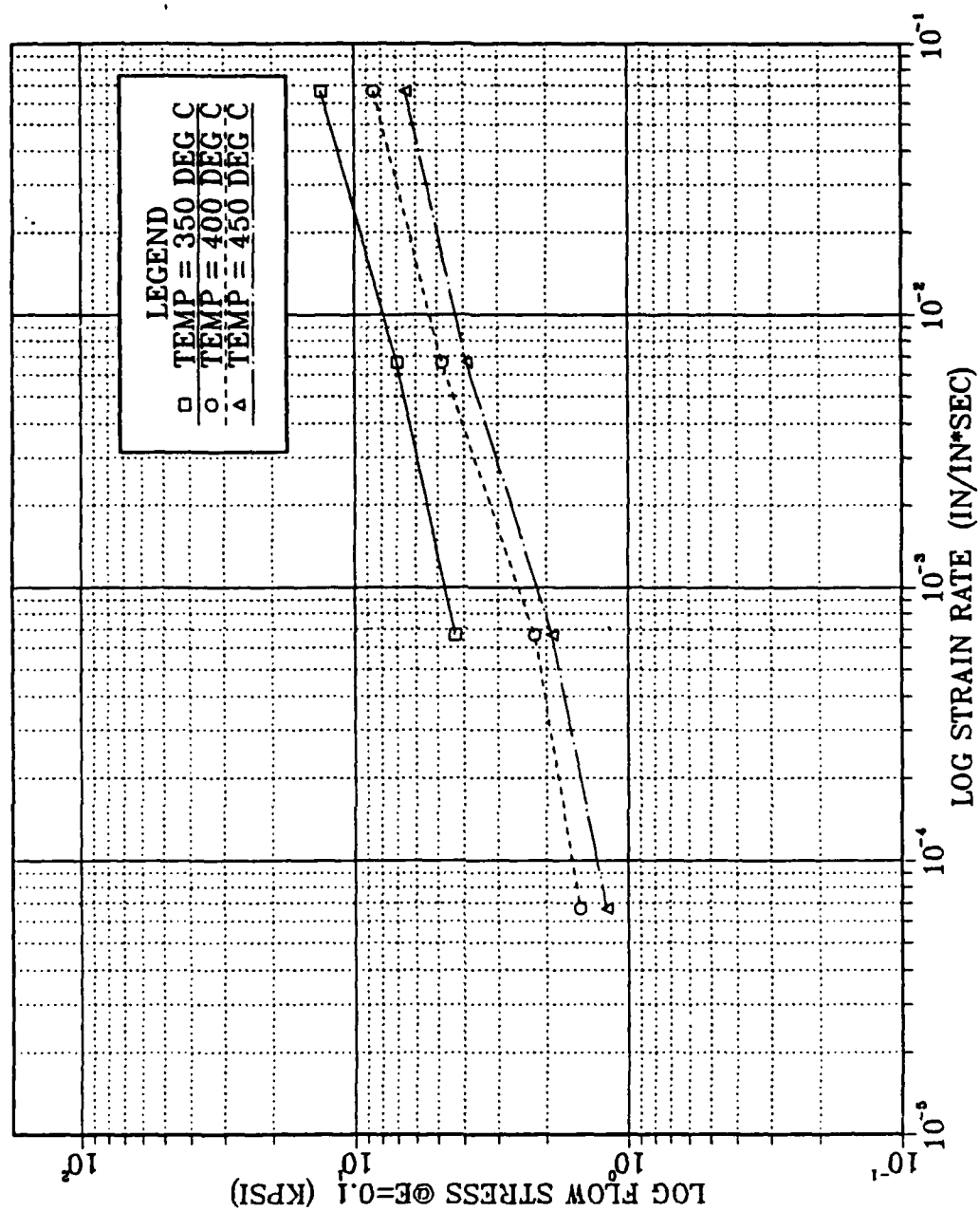


Figure 18. TMP B Strain rate sensitivity (m): $m \approx 0.3$ at temperatures of 400°C.

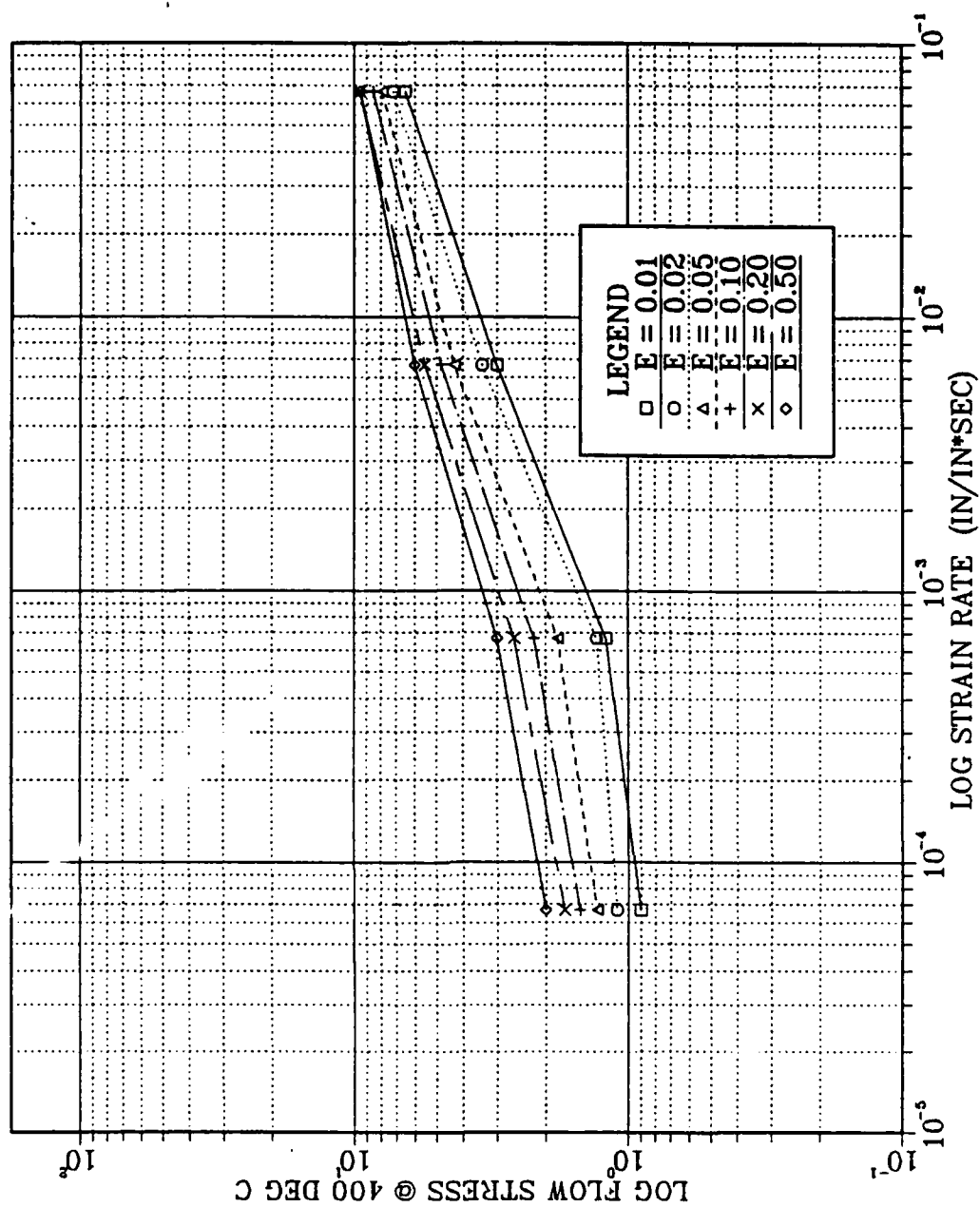


Figure 19. TMP B Variation of strain rate sensitivity: Strain rate sensitivity varies as the sample strains due to grain coarsening. At 1% strain $m \approx 0.4$, reducing to $m \approx 0.25$ at 50% strain.

therefore suggest extension of continuous recrystallization. This phenomenon was also observed in the strain rate sensitivity coefficient. It was seen that the value of the strain rate sensitivity coefficient decreased as the sample was strained (Figure 19). This phenomenon may be attributed to grain coarsening, especially at lower strain rates, reflecting greater times at test temperature. At strains beyond a maximum point, the flow stress decreased. This may reflect microstructural softening or the onset of diffuse necking. This detail of the stress strain curve was not examined further in this work.

The microstructure of NAVALITE processed by TMP B reveals a highly refined microstructure in the 'as rolled' condition. The precipitate is present in a uniform dispersion and is fine in size. There is banding in the processed microstructure (Figure 20). The grip section of a tested tensile specimen details the banding along the long transverse axis (Figure 21).

Superplastic forming appeared to enhance precipitate growth and some grain coarsening has probably occurred with the precipitation growth of some samples (Figure 22). Also, some cavitation has become apparent in the necked region.

TMP E, with a step down rolling temperature of 20°C, resulted in severe edge cracking in the final rolled strip. Some testing samples were salvageable and tested. The microstructure appears to be as well refined as that of TMP B as shown by examination of the sample grip section (Figure 23). The ductility was virtually the same as TMP B. Another portion of the rolled strip was examined and revealed cracks forming due to the low temperature (Figure 24).

D. INTERPRETATION OF RESULTS

In the ternary Al-Mg-Li alloy system, NAVALITE lies in a quasi-binary section with constituents being the Al solid solution and δ' (Al_3Li) or δ (Al_2LiMg). The δ -phase is believed to be the precipitate which stabilizes the microstructure during continuous recrystallization. Previous work in the Al-Mg alloy system identified the β -phase precipitate as interacting with dislocations during continuous recrystallization. It is recognized that the manner in which the δ -phase interacts with the subgrain structure during thermomechanical processing may be different from that of the β due to the different chemical makeup and morphology.

Initially, it must be determined if, in fact, TMP as performed in this research produced δ . The δ' produced peak hardness by solution treatment at 120-170°C after a period of 12 hours, from which the δ' formed δ . The very fine and spherically shaped coherent δ' -phase would not likely interact with substructure triple junctions effectively.



Figure 20. TMP B 'as rolled': NAVALITE after TMP B in the 'as rolled' condition. Precipitate dispersion is fine and uniformly distributed. Slight banding has occurred during warm rolling. (55X)

It is probable that TMP using 300°C anneals, with a total annealing time of six hours, did produce δ . If in fact this δ -phase was produced, the question remains if it was produced early in the TMP where maximum benefits could be realized.

The β -phase of the Al-Mg alloy system is an incoherent intermetallic which can be refined during processing to a size of 0.2 to 0.5 μm . In this form the β -phase interacts with dislocation structures, stabilizing them during TMP. The coarsely dispersed rod-shaped δ intermetallic is slightly larger, about 2.0 μm . The size distribution of the second phase is considered important in order that a sufficient number of the precipitate particles be of adequate size to ensure stabilization of the subgrain structure during TMP. A narrow size distribution by process control may be important in optimizing grain refinement and should be investigated. [Ref. 3: p. 113]

From this research, it can be deduced that the solvus temperature of the δ -phase is higher than 400°C for this alloy, whereas that of β is $\approx 360^\circ\text{C}$ for 10wt.pct.Mg. For NAVALITE at higher temperatures, there is likely to be enhancement of grain growth during superplastic forming. The possibility of cavitation is increased during forming at higher temperatures as well.

Peak ductilities for all TMP's conducted on NAVALITE were obtained when tested at a temperature of 400°C and at a strain rate of $6.67 \times 10^{-4} \text{ s}^{-1}$. As compared to work in



Figure 21. TMP B grip section: The undeformed grip section after SPDF showing the banding introduced during TMP. (220X)

high-Mg, Aluminum-Magnesium systems, consistent peaks were obtained by Munroe at lower temperatures (300-325°C) and higher strain rates ($6.67 \times 10^{-3} \text{ s}^{-1}$) [Ref. 13]. This shift is believed to have resulted from increasing diffusion combined with grain coarsening (which suppresses the superplastic mechanism). Peak strains are likely the result of microstructural coarsening which resulted from prolonged periods at test temperature.

Optical microscopy revealed a refined grain structure in NAVALITE nearly identical to that of the high Mg Aluminum-Magnesium alloys. This observation coupled with the high ductilities in the 400 percent range would suggest that the structure evolved as proposed by Hales and McNelley [Ref. 9: p. 1238]. It is likely that the evolving dislocation substructure in the Al-Mg-Li system where δ is the stabilizing structure is coarser than that in the binary Al-Mg system where β provides stabilization. It is likely, however, that sub boundaries have not achieved misorientations as great as those attained with the Al-Mg alloys.

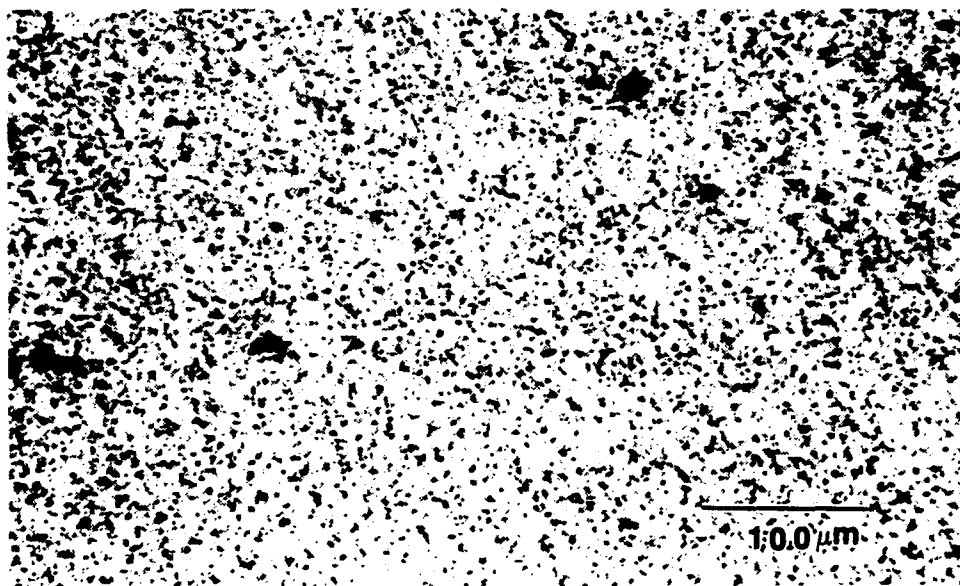


Figure 22. TMP B necked region: In the highly deformed region, precipitation coalescence and grain growth have occurred. Cavitation appears as dark spots. (220X)



Figure 23. TMP E grip section: A highly refined microstructure comparable to TMP B grip section in Figure 21. (220X)



Figure 24. TMP E as rolled: Taken from a different location in the rolled strip than that of the sample in figure 23, interior fractures reveal a microstructure of internal fractures. (55X)

The focus of this research was the effects of increased dislocation density which could be produced during TMP by rolling at a reduced temperature. Attempts to improve ductilities substantially beyond 400% were not successful. Superplastic response of a material will vary depending on the TMP used to produce refinement of the substructure, the nature and misorientation of the grain boundaries and the presence of a stabilizing second phase precipitate. Before considering a material for superplastic behavior, the composition must be that of a two phase structure in order to suppress grain growth. Secondly, total strain, annealing time, annealing temperature and rolling temperature must be properly chosen to realize maximum gains from TMP. Results from this research are that optimum conditions for realizing ductilities in excess of 400% have not been found. However, that ductilities in the range of 400% is a significant finding. Ductilities of this magnitude would not be expected due to the composition of the alloy only. TMP has enhanced the superplasticity of NAVALITE by conditioning the microstructure. Control over the microstructure by TMP variables has been demonstrated. The nature of the mechanism which control grain refinement, grain boundary misorientation and adequacy of the second phase are not fully understood at this time and should be the area of further research.

V. CONCLUSIONS

1. NAVALITE is capable of superplastic deformation after thermomechanical processing. Maximum ductility achieved was 428%.
2. Refinement of microstructure by TMP using reduced temperature rolling in conjunction with 30 minute anneals was minimal.
3. Strain rate sensitivity coefficient, m , was approximately equal to 0.3 for temperatures of 400°C at strain rates of $6.67 \times 10^{-4} \text{ s}^{-1}$.
4. Strain rate sensitivity during deformation decreases due to grain growth.
5. Maximum ductilities were obtained in all cases at a deformation temperature of 400°C and a strain rate of $6.67 \times 10^{-4} \text{ s}^{-1}$.

VI. RECOMMENDATIONS FOR FURTHER STUDY

1. Investigate time/temperature variations in annealing during TMP.
2. Investigate low temperature rolling in conjunction with a higher annealing temperature and different annealing time.
3. Investigate tensile testing in a non-reactive atmosphere.
4. Determine phase transition temperatures with Differential Scanning Calorimetry (DSC).
5. Investigate microstructure with Transmission Electron Microscopy (TEM).

APPENDIX A. DUCTILITIES (PCT. ELONG.) OF TMP C, D AND E

Table 6. DUCTILITY (% ELONG.) OF MATL. PROCESSED WITH TMP C

	350°C	400°C	450°C
$6.67 \times 10^{-2} \text{ s}^{-1}$	172	193	229
$6.67 \times 10^{-3} \text{ s}^{-1}$	172	331	225
$6.67 \times 10^{-4} \text{ s}^{-1}$	175	363	181
$6.67 \times 10^{-5} \text{ s}^{-1}$	---	197	---

Table 7. DUCTILITY (% ELONG.) OF MATL. PROCESSED WITH TMP D

	350°C	400°C	450°C
$6.67 \times 10^{-2} \text{ s}^{-1}$	172	200	197
$6.67 \times 10^{-3} \text{ s}^{-1}$	322	253	253
$6.67 \times 10^{-4} \text{ s}^{-1}$	191	387	187
$6.67 \times 10^{-5} \text{ s}^{-1}$	---	335	---

Table 8. DUCTILITY (% ELONG.) OF MATL. PROCESSED WITH TMP E

	350°C	400°C	450°C
$6.67 \times 10^{-2} \text{ s}^{-1}$	---	275	---
$6.67 \times 10^{-3} \text{ s}^{-1}$	---	303	---
$6.67 \times 10^{-4} \text{ s}^{-1}$	209	425	287
$6.67 \times 10^{-5} \text{ s}^{-1}$	---	250	---

APPENDIX B. TRUE STRESS VS. TRUE STRAIN CURVES

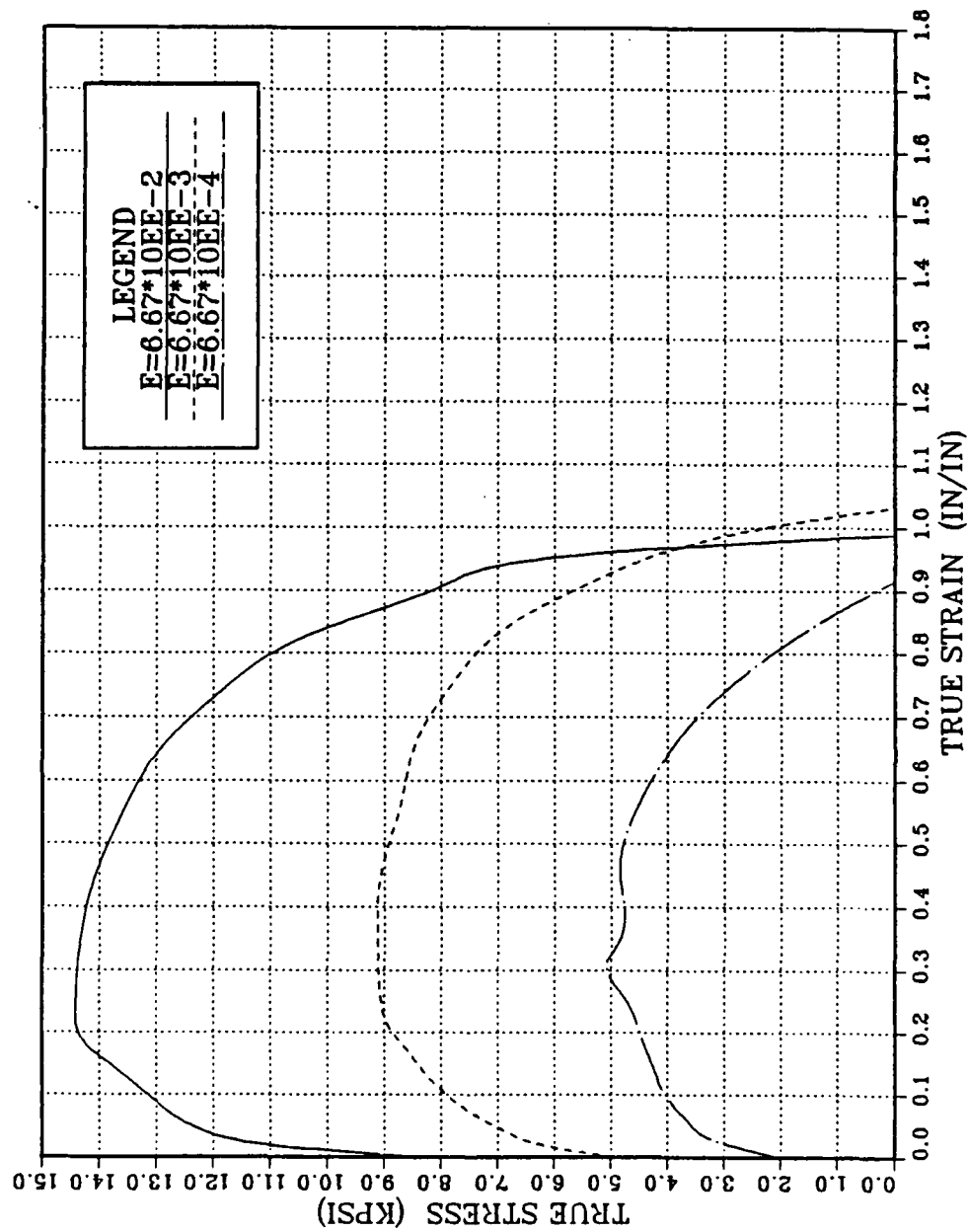


Figure 25. Stress Strain Curve for TMP A: True stress vs. true strain taken for various strain rates at 350°C.

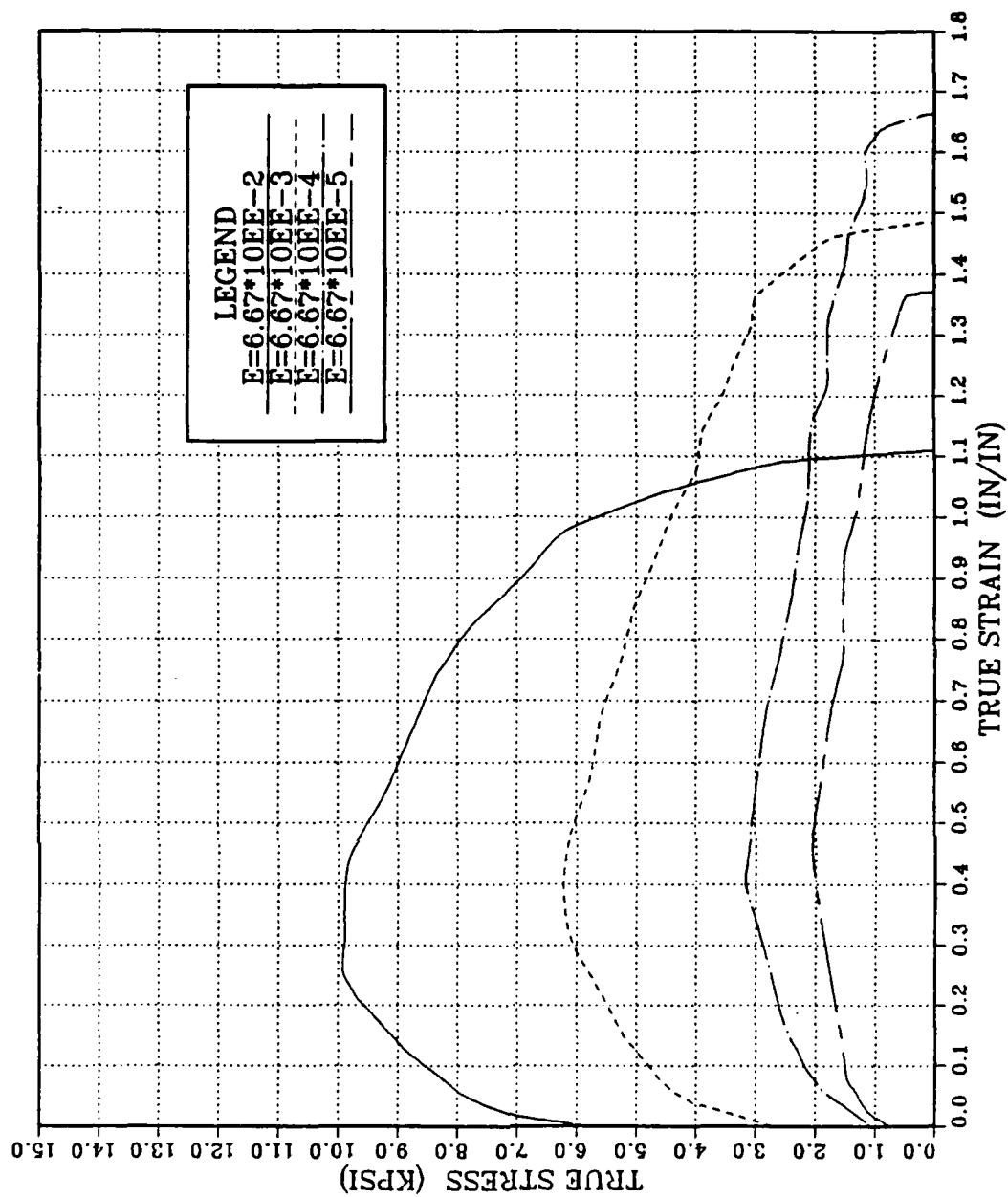


Figure 26. Stress Strain Curve for TMP A: True stress vs. true strain taken for various strain rates at 400°C.

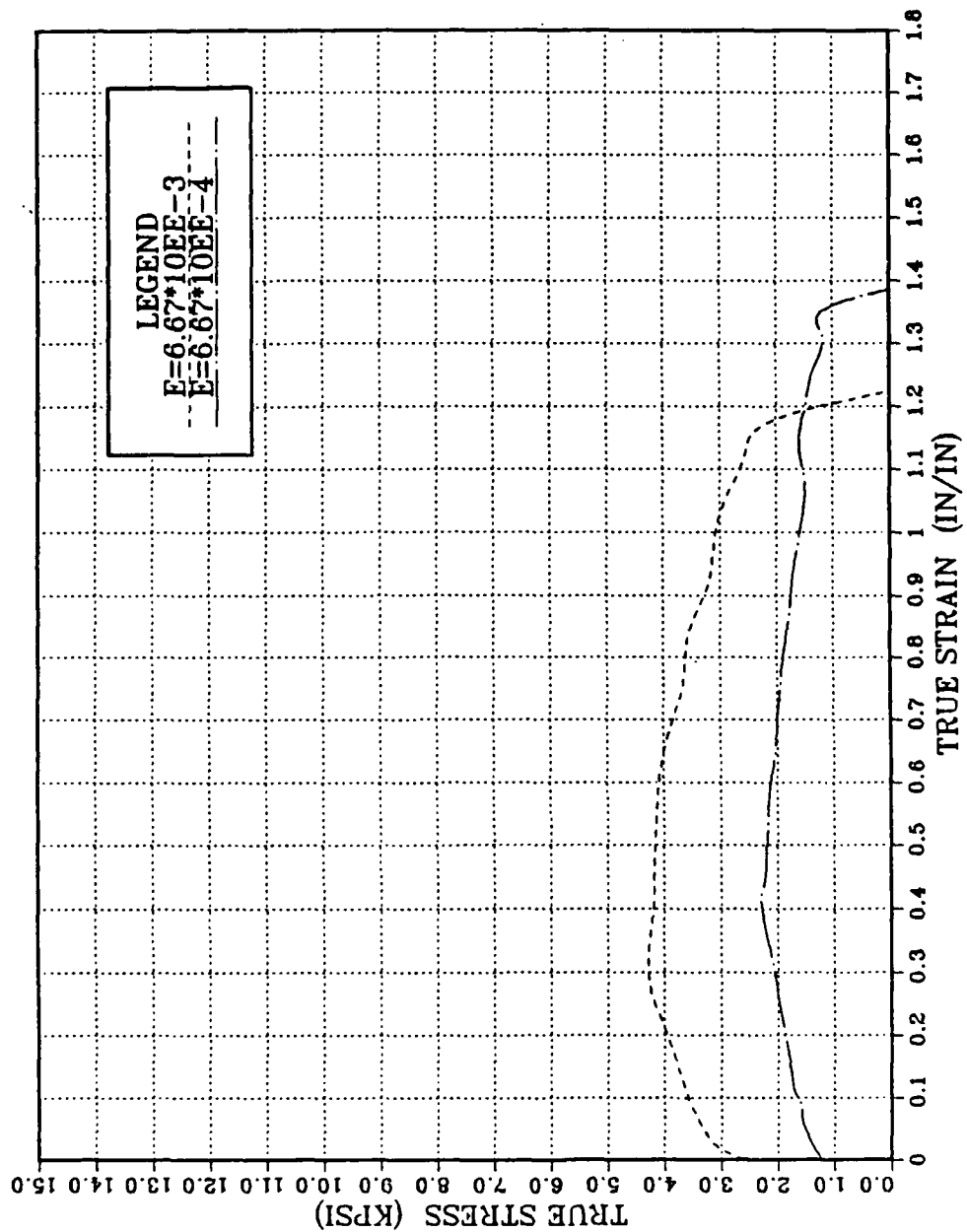


Figure 27. Stress Strain Curve for TMP A: True stress vs. true strain taken for various strain rates at 450°C.

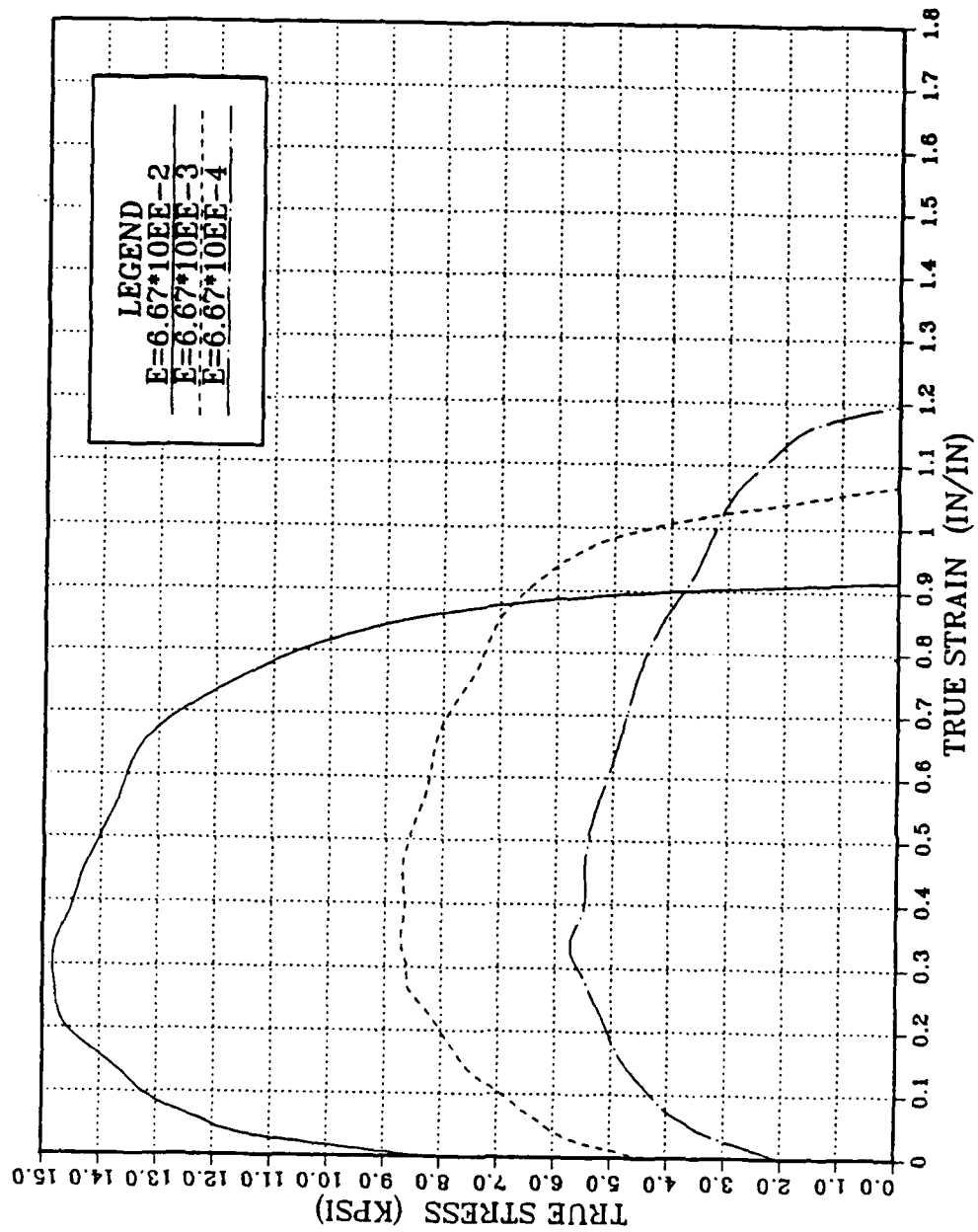


Figure 28. Stress Strain Curve for TMP B: True stress vs. true strain taken for various strain rates at 350°C.

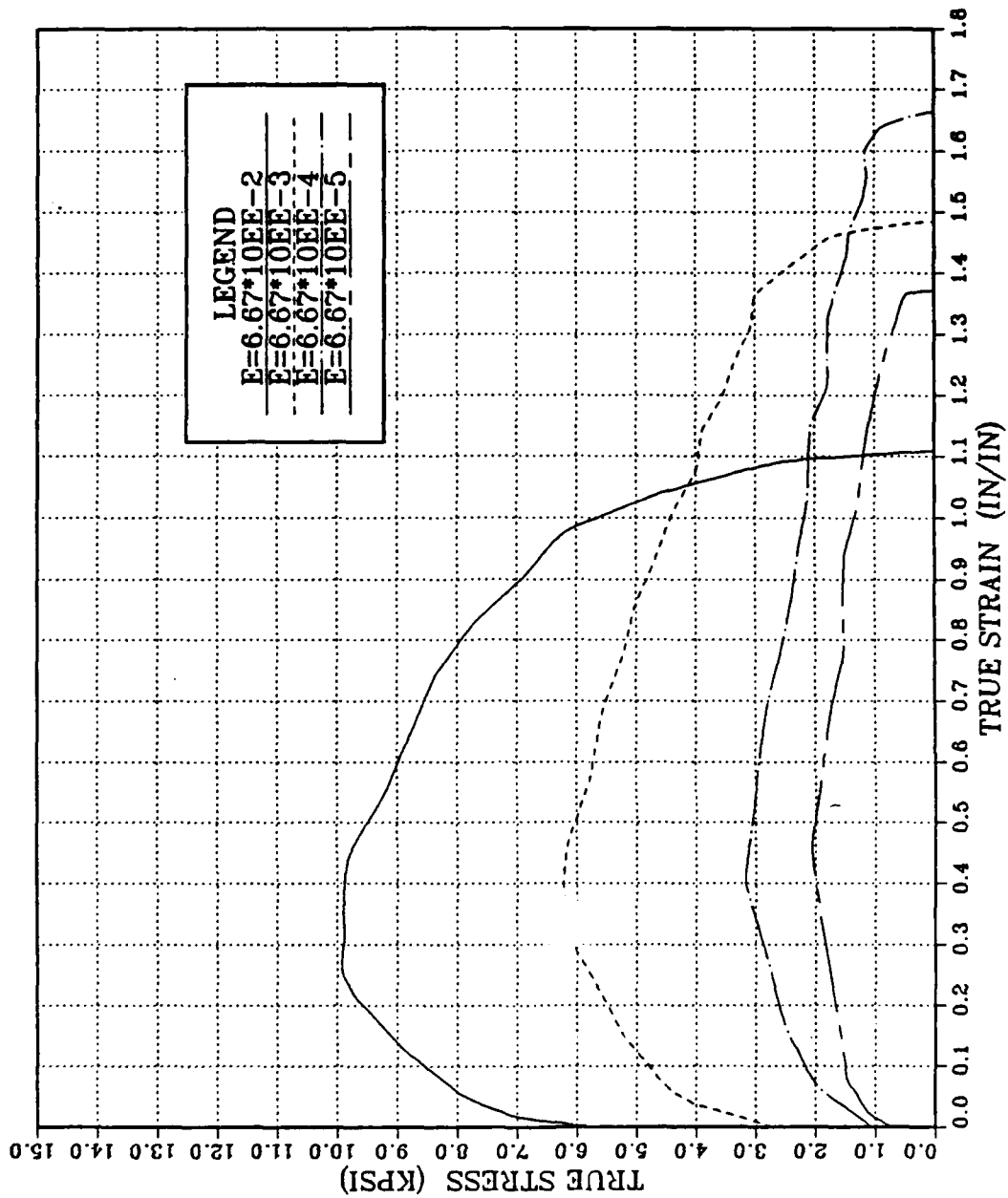


Figure 29. Stress Strain Curve for TMP B: True stress vs. true strain taken for various strain rates at 400°C.

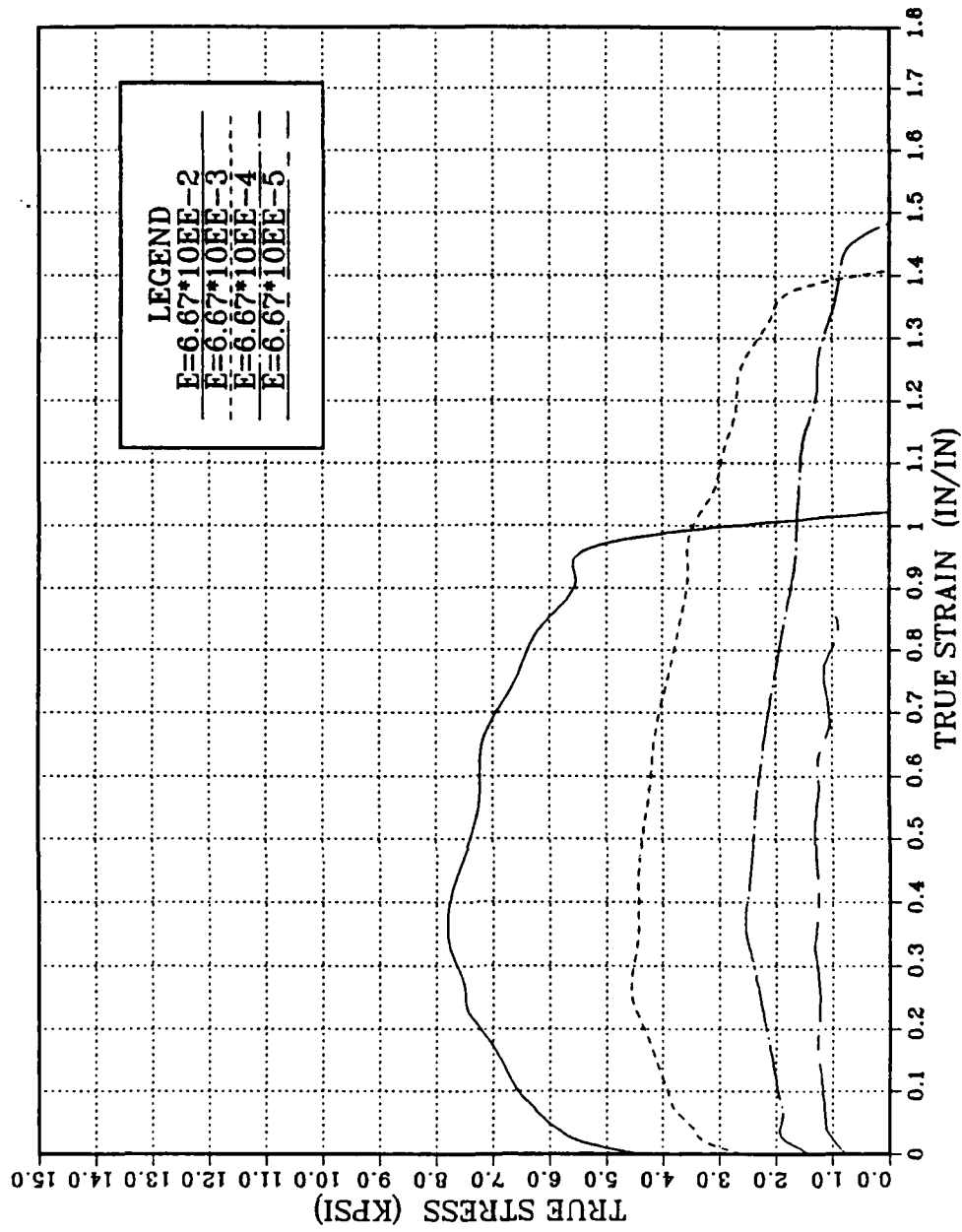


Figure 30. Stress Strain Curve for TMP B: True stress vs. true strain taken for various strain rates at 450°C.

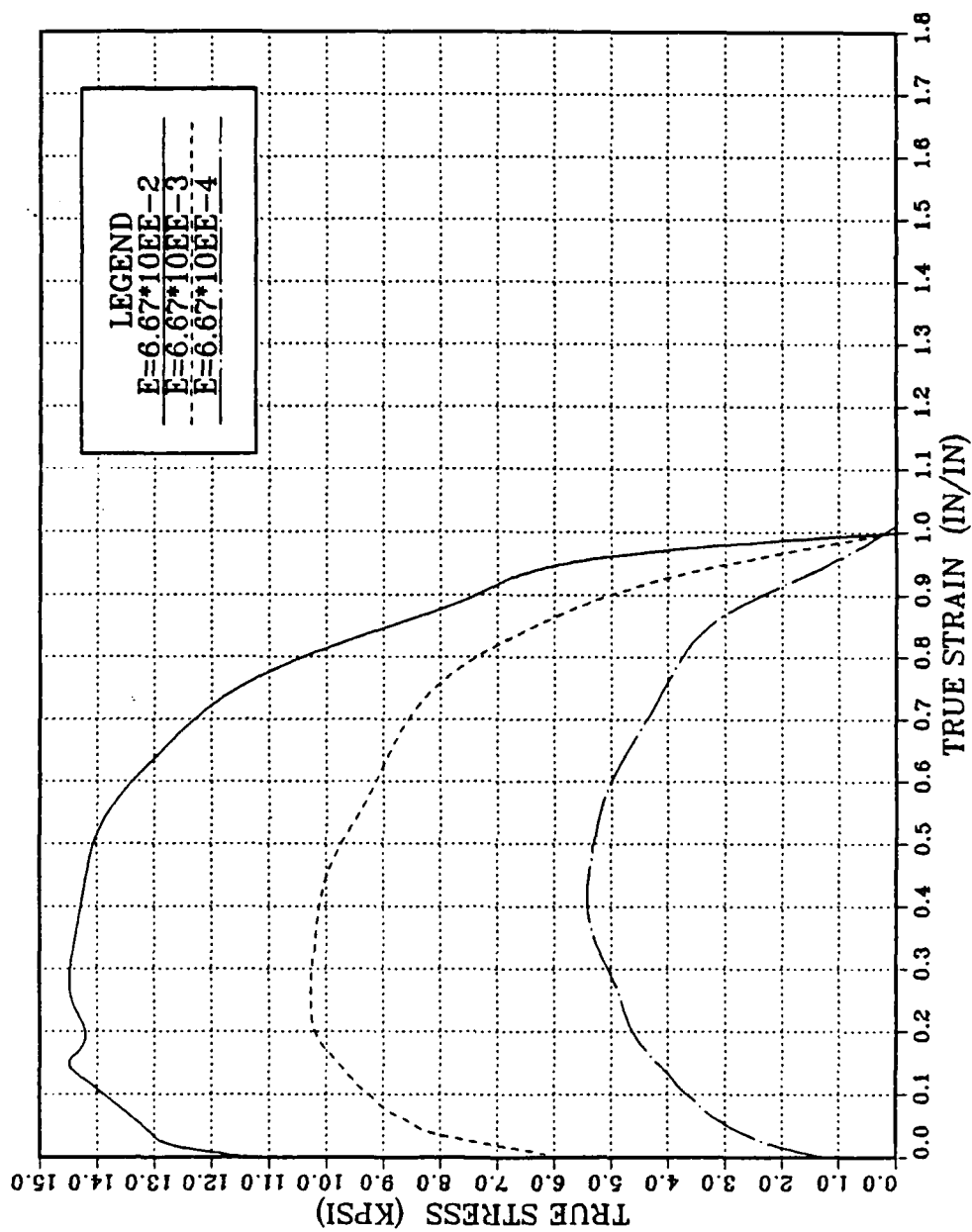


Figure 31. Stress Strain Curve for TMP C: True stress vs. true strain taken for various strain rates at 350°C.

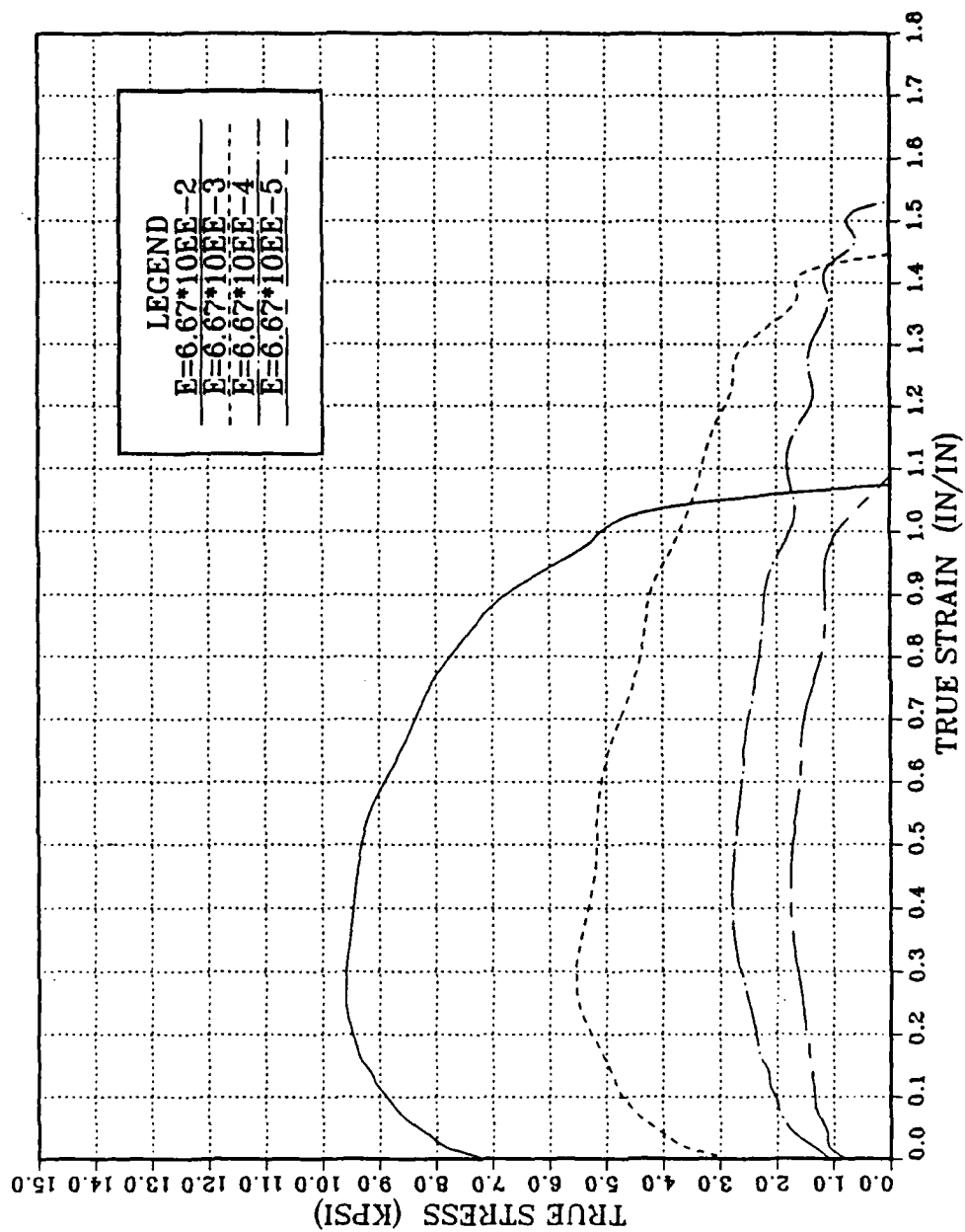


Figure 32. Stress Strain Curve for TMP C: True stress vs. true strain taken for various strain rates at 400°C.

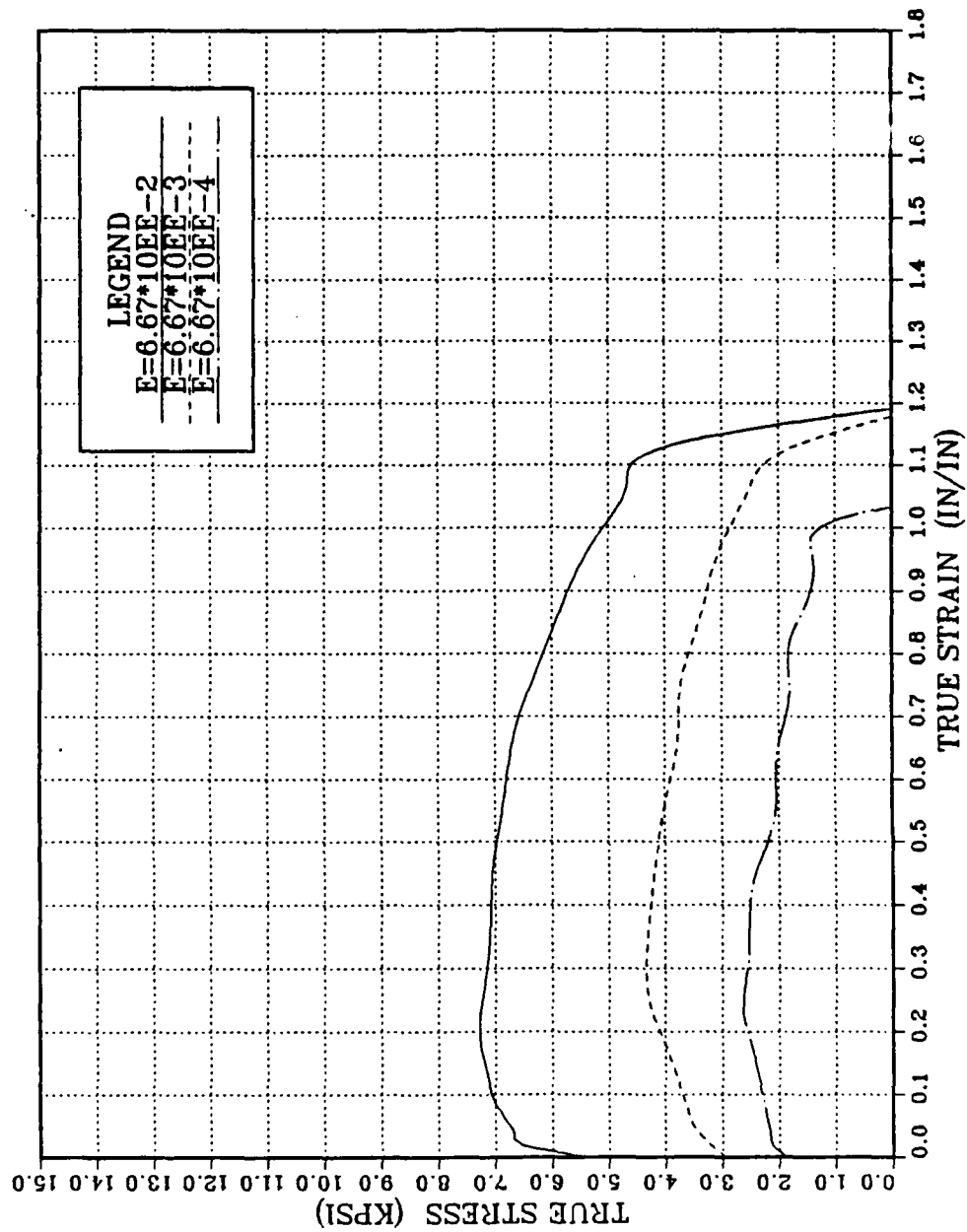


Figure 33. Stress Strain Curve for TMP C: True stress vs. true strain taken for various strain rates at 450°C.

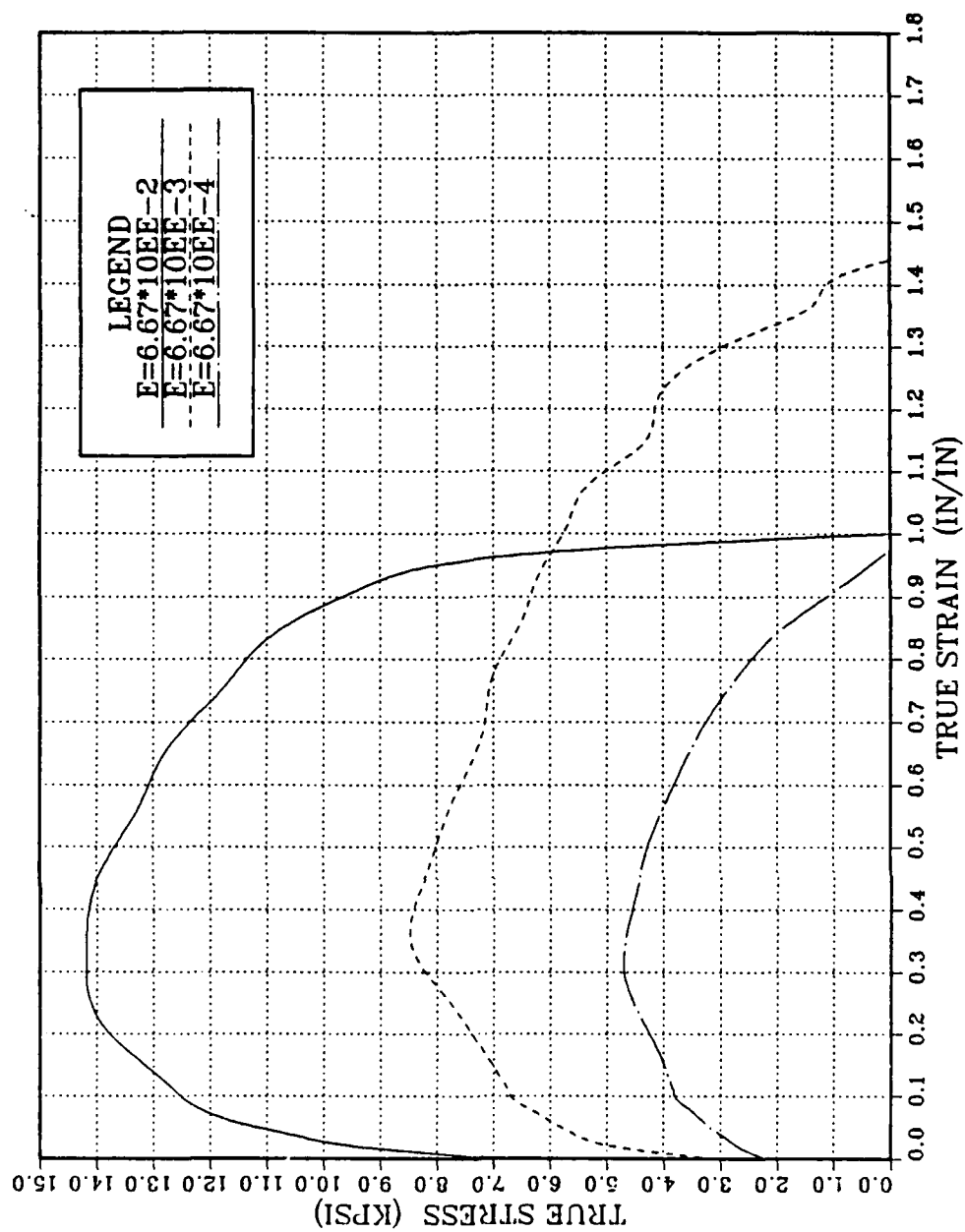


Figure 34. Stress Strain Curve for TMP D: True stress vs. true strain taken for various strain rates at 350°C.

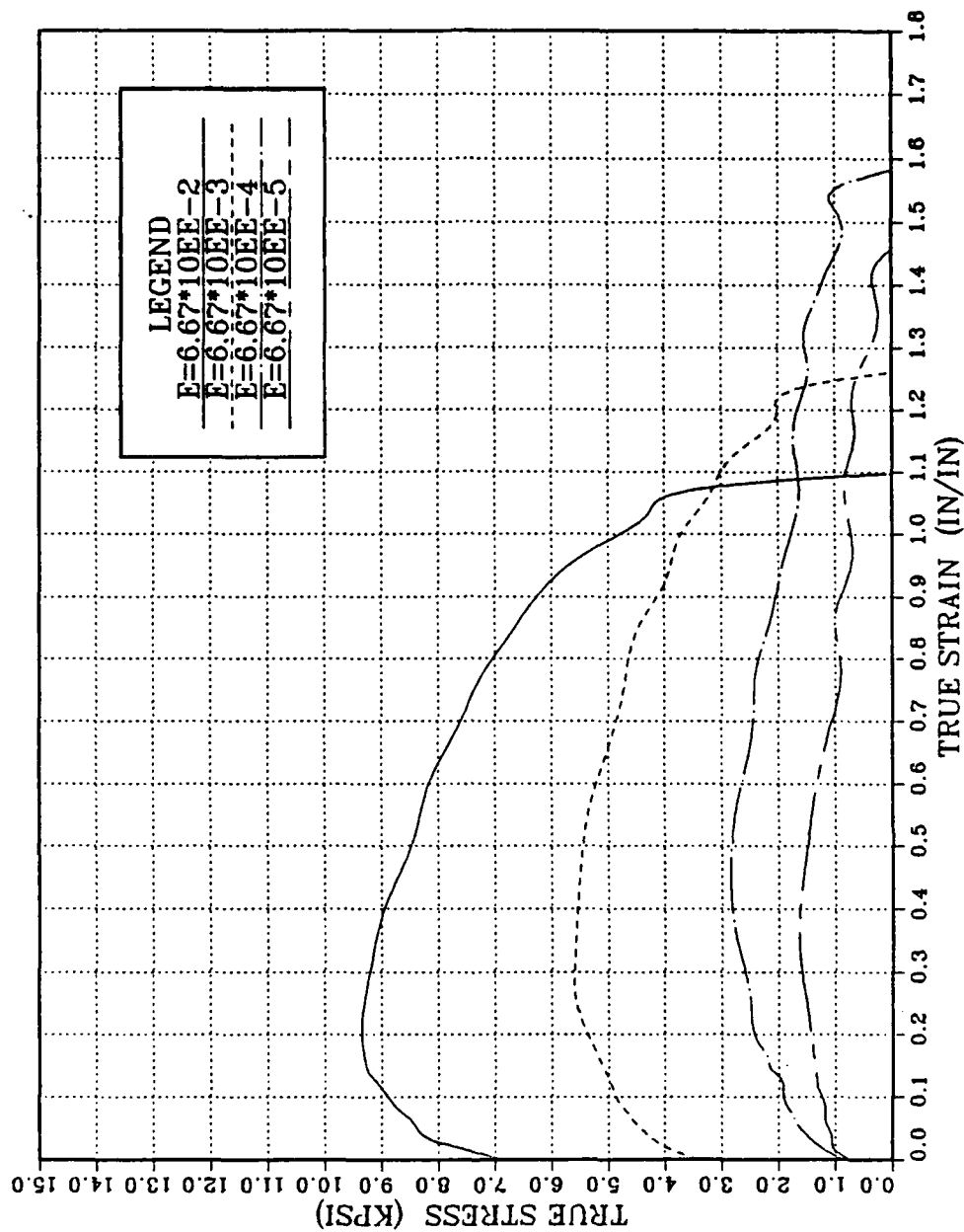


Figure 35. Stress Strain Curve for TMP D: True stress vs. true strain taken for various strain rates at 400°C.

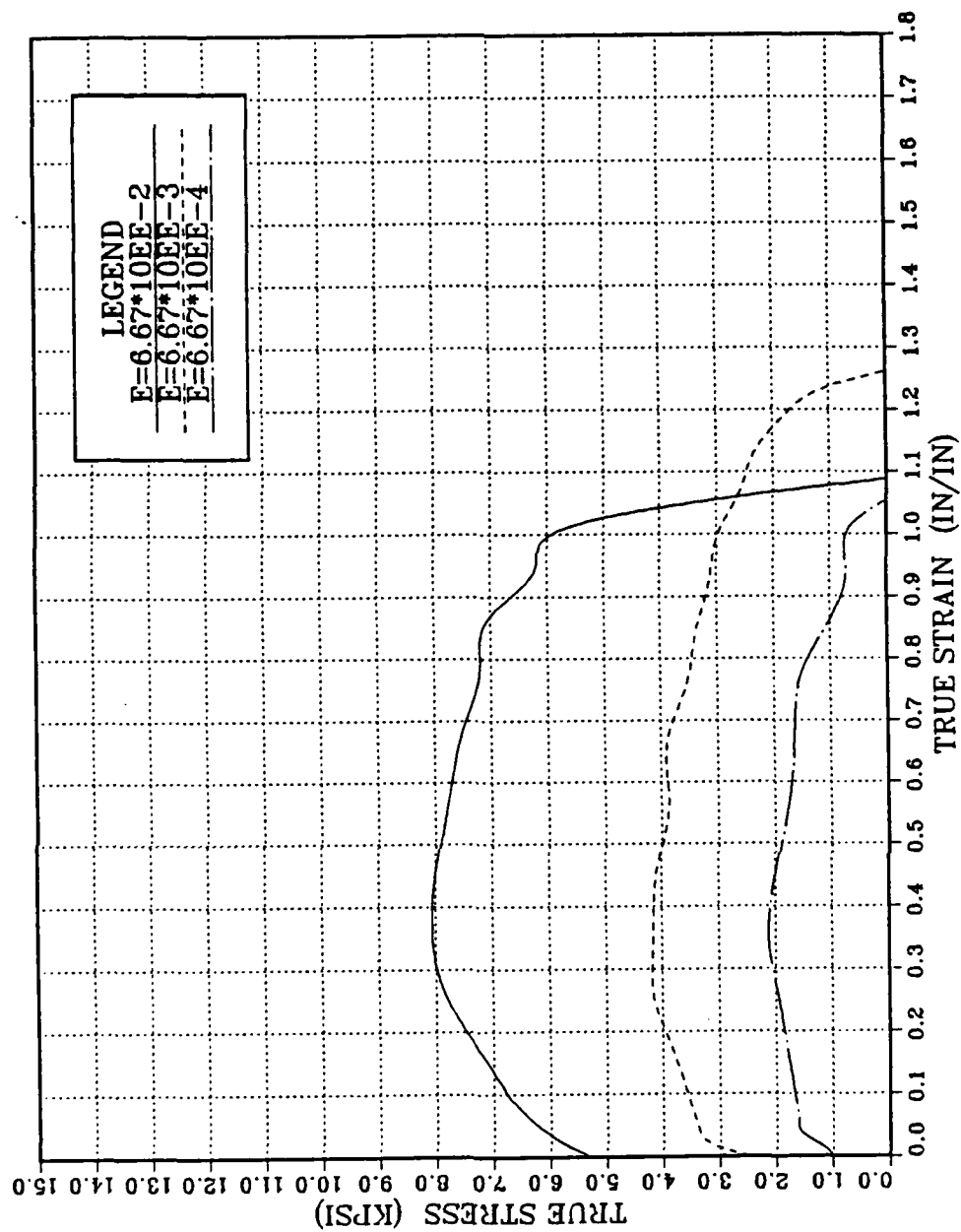


Figure 36. Stress Strain Curve for TMP D: True stress vs. true strain taken for various strain rates at 450°C.

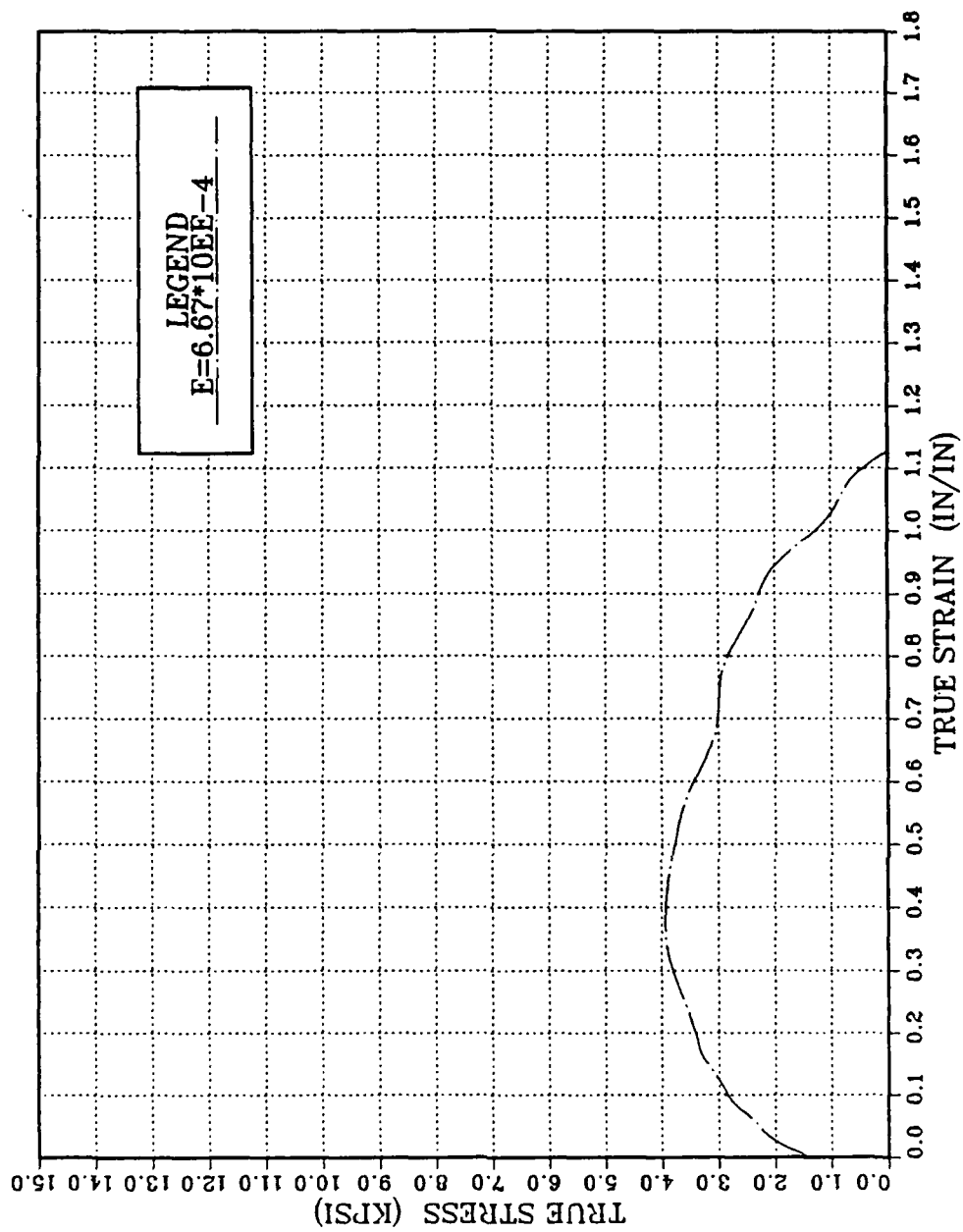


Figure 37. Stress Strain Curve for TMP E: True stress vs. true strain taken for various strain rates at 350°C.

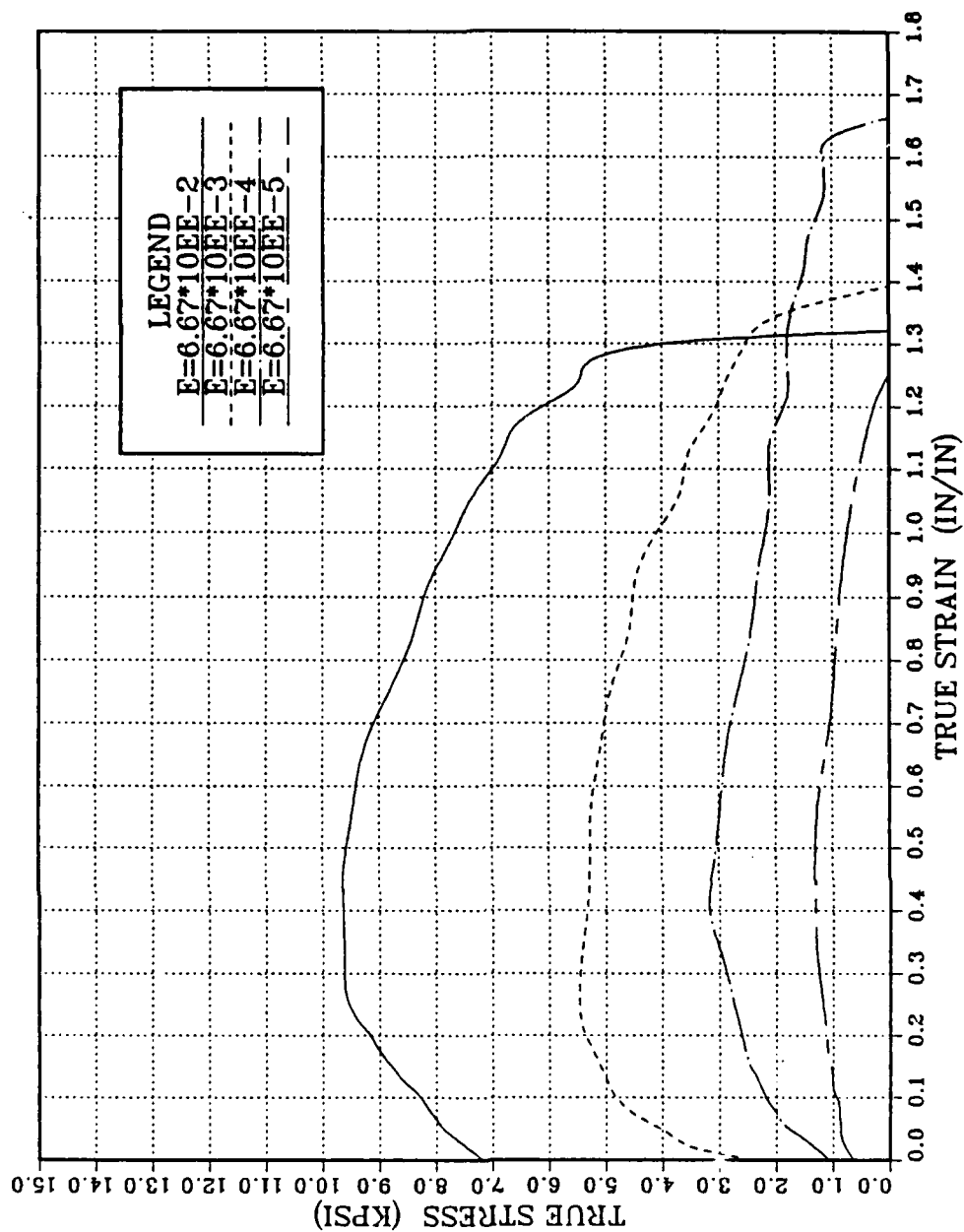


Figure 38. Stress Strain Curve for TMP E: True stress vs. true strain taken for various strain rates at 400°C.

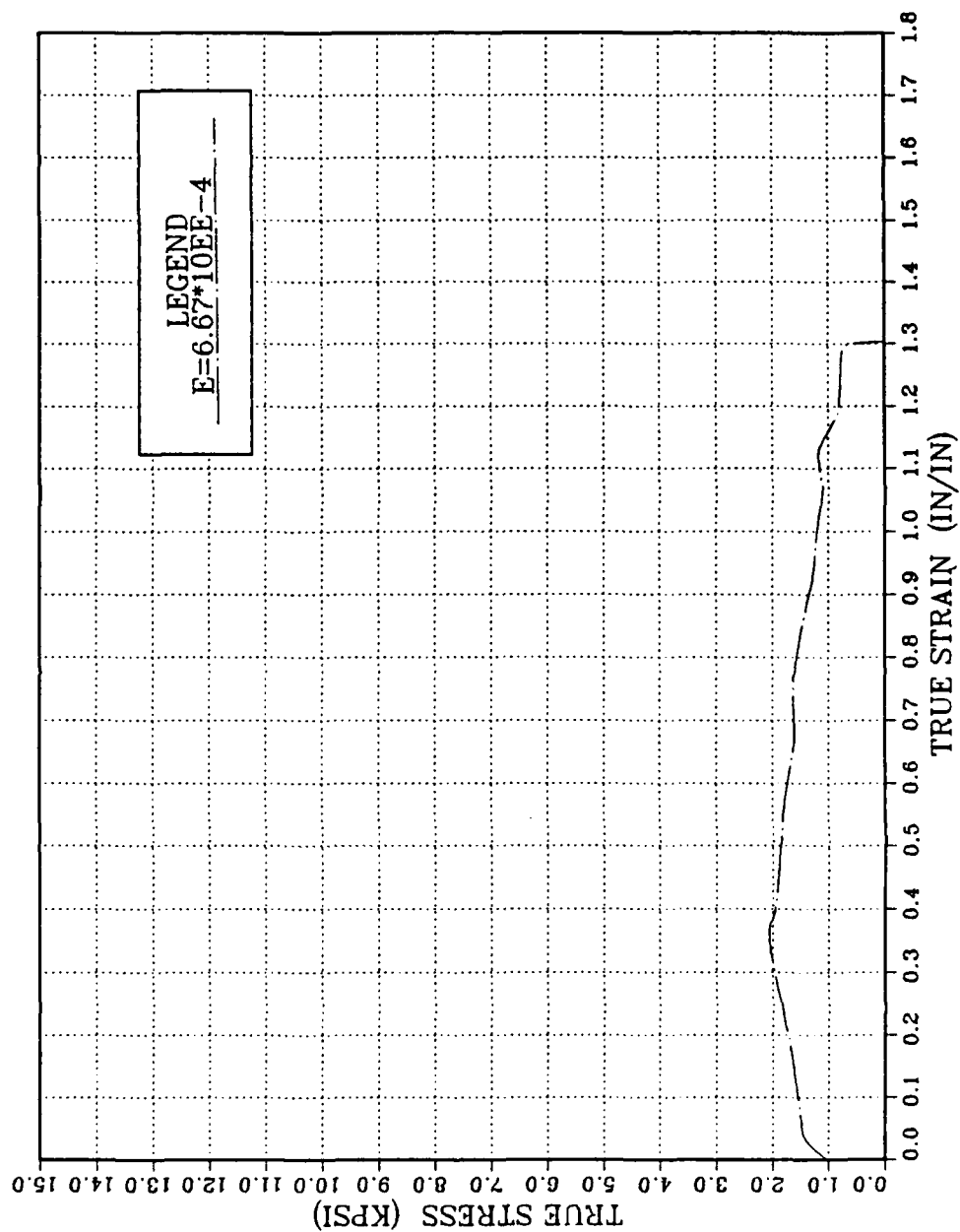


Figure 39. Stress Strain Curve for TMP E: True stress vs. true strain taken for various strain rates at 450°C.

APPENDIX C. STRAIN-RATE SENSITIVITY FOR TMP A, C, D, AND E

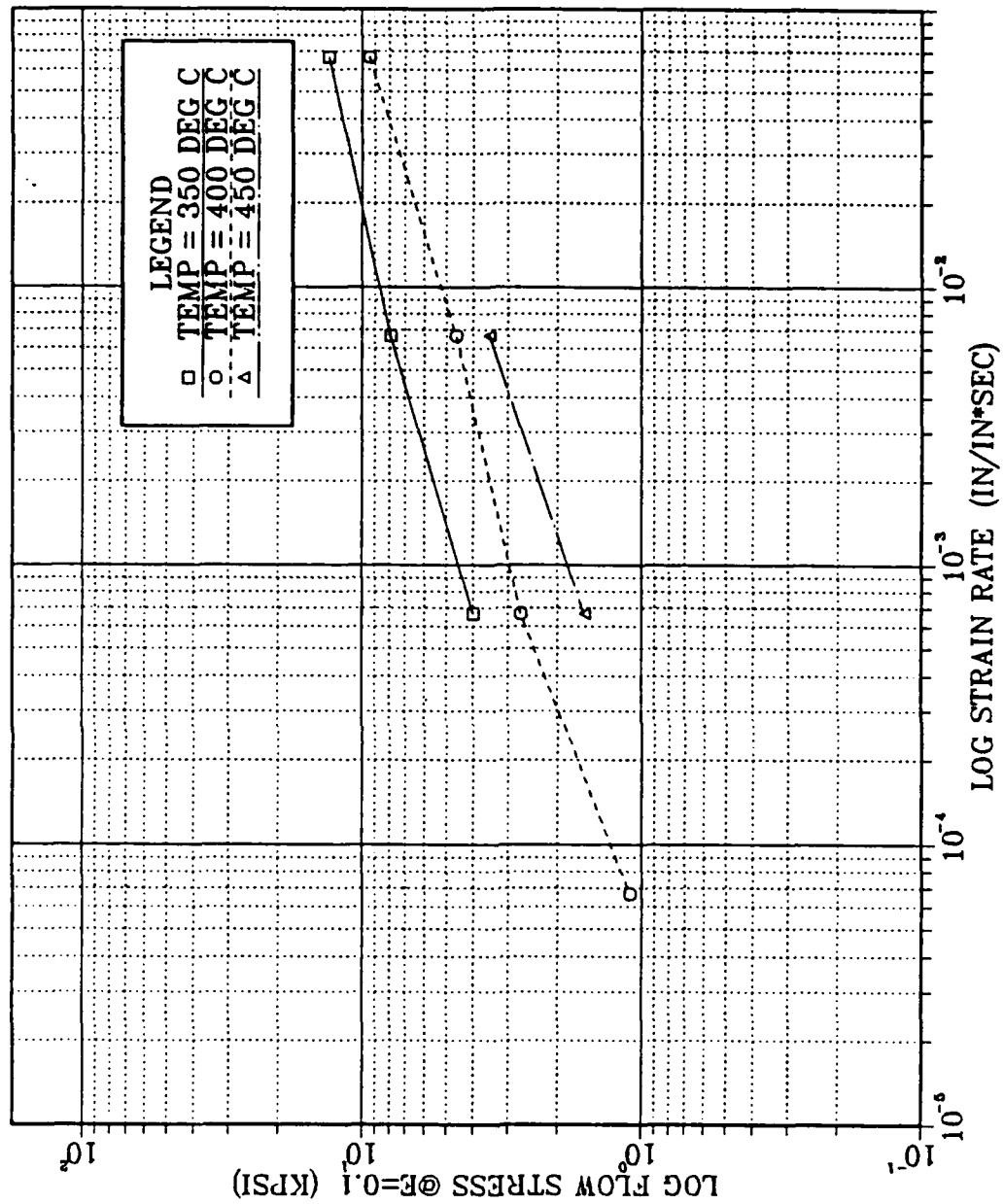


Figure 40. TMP A Strain rate sensitivity (m): $m \approx 0.3$ at temperatures of 400°C.

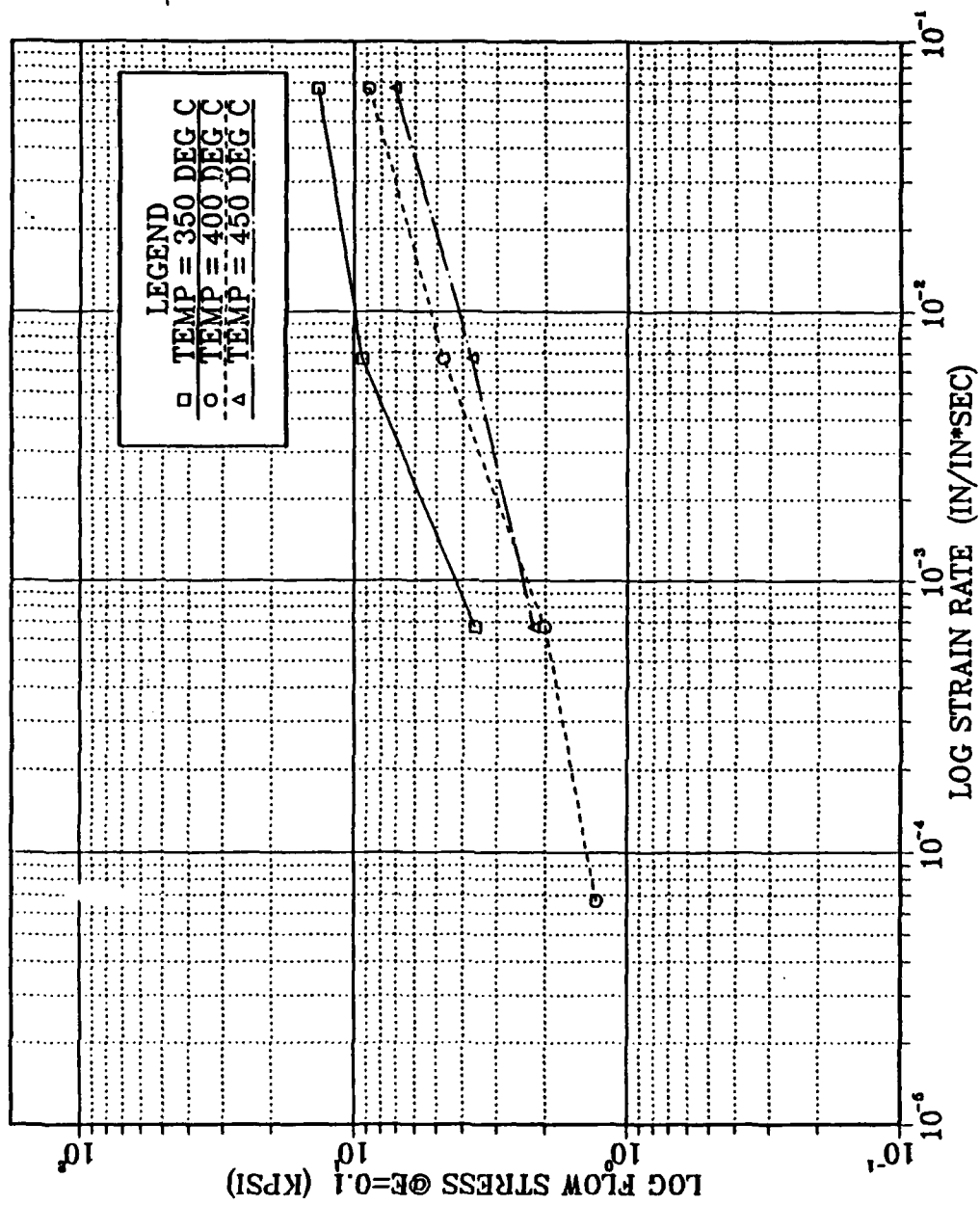


Figure 41. TMC Strain rate sensitivity (m): $m \approx 0.3$ at temperatures of 400°C.

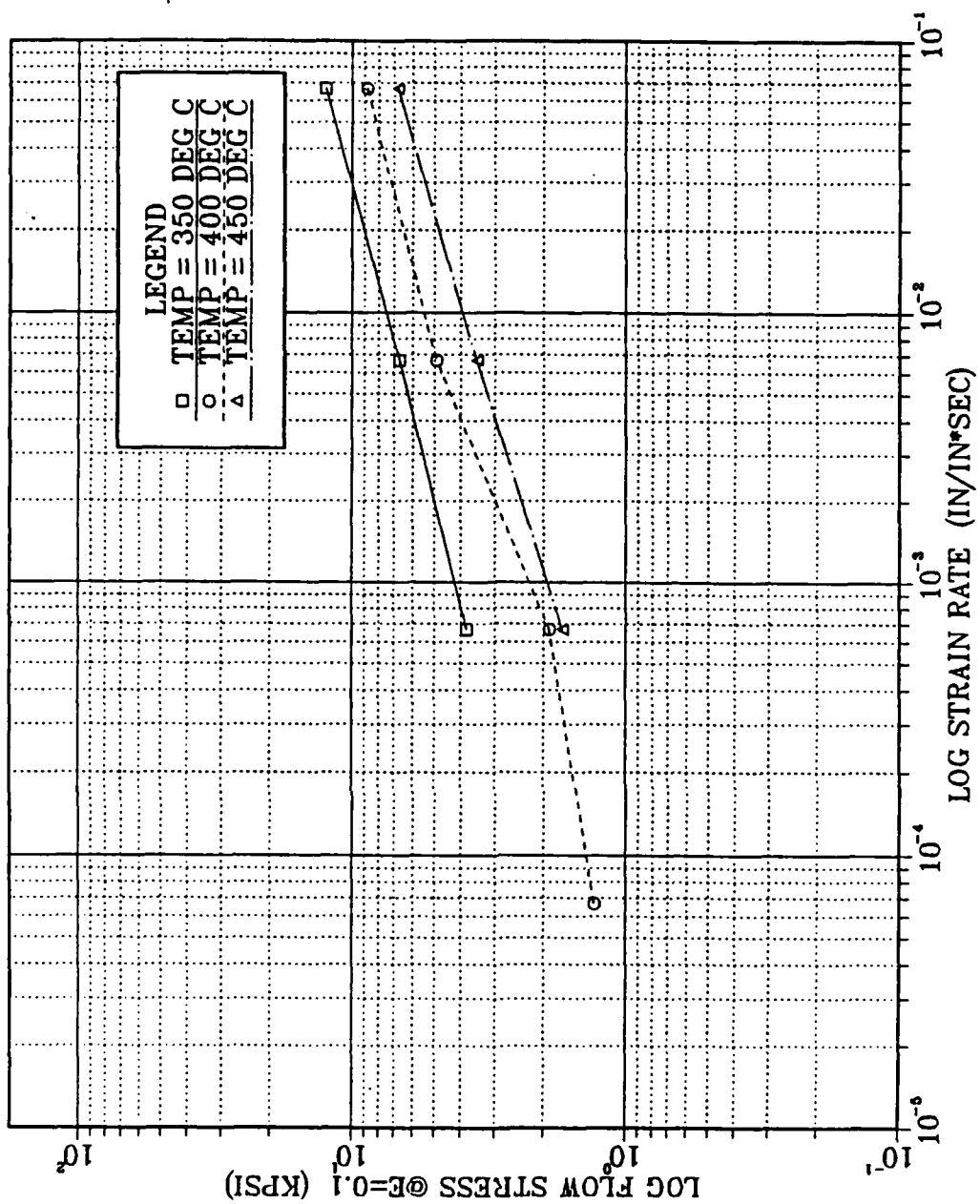


Figure 42. TMD Strain rate sensitivity (m): $m \approx 0.3$ at temperatures of 400°C.

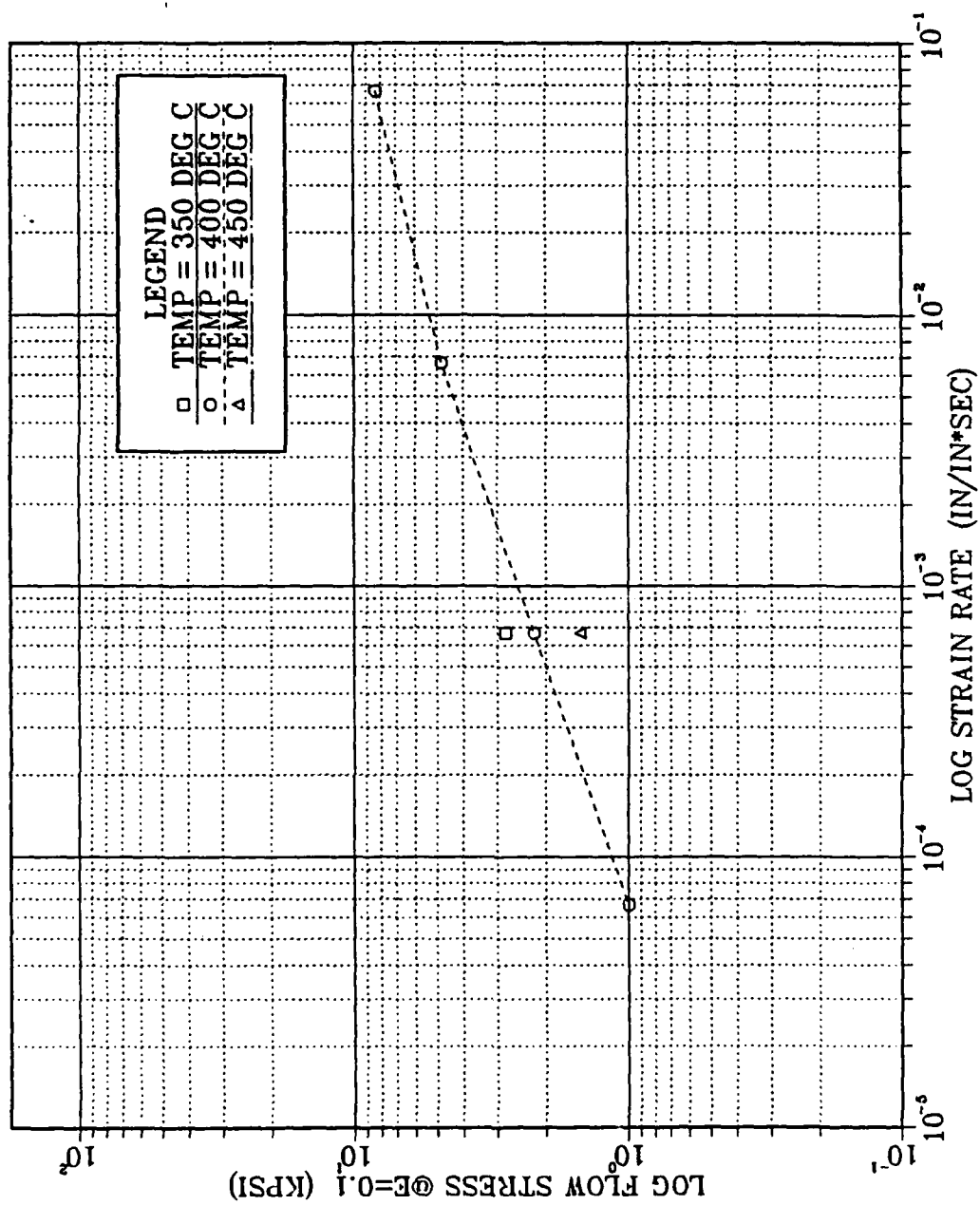


Figure 43. Tmp E Strain rate sensitivity (m): $m \approx 0.3$ at temperatures of 400°C.

APPENDIX D. VARIATION OF STRAIN-RATE SENSITIVITY FOR TMP A, C, D, AND E

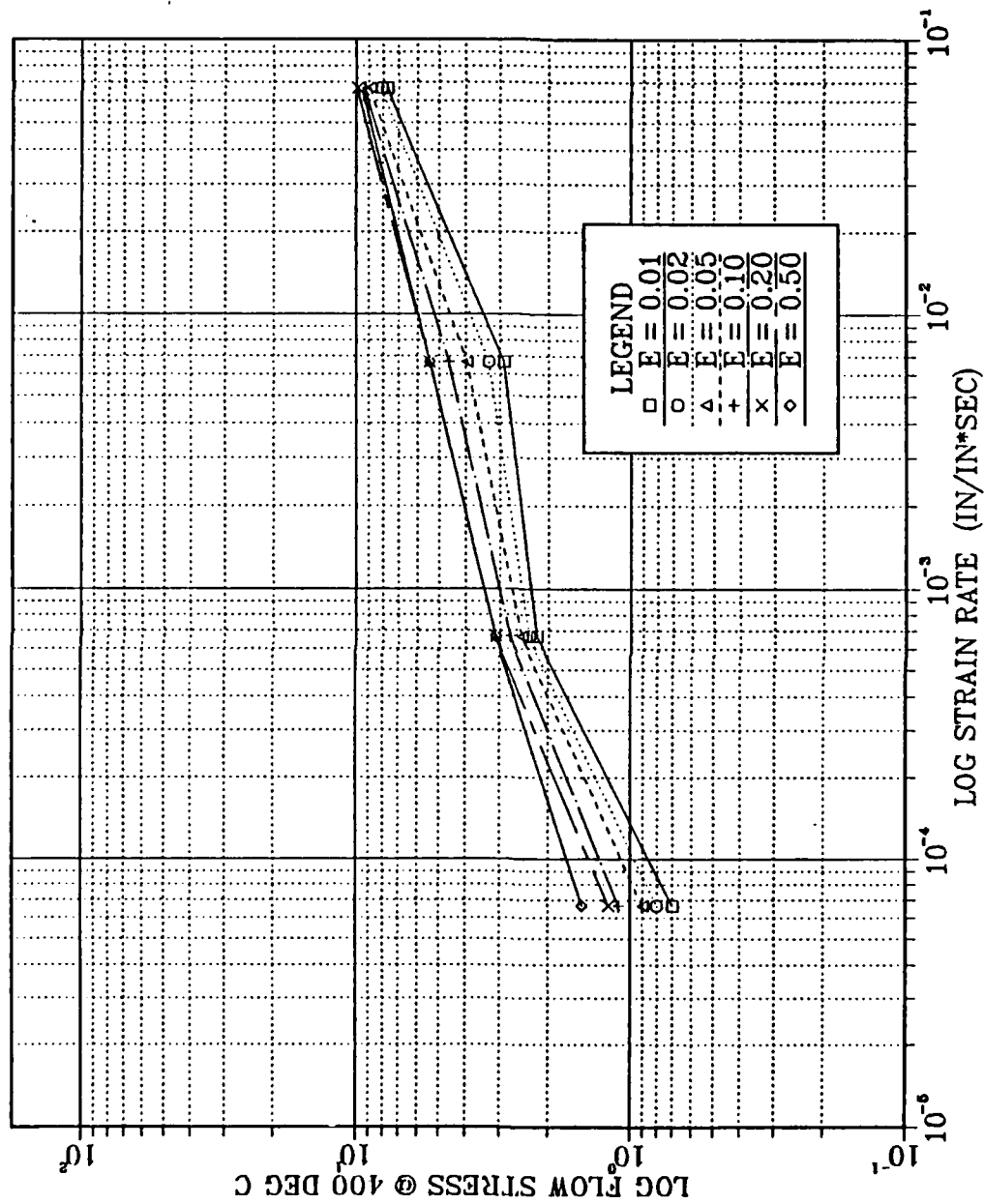


Figure 44. TMP A Variation of strain rate sensitivity: Strain rate sensitivity varies as the sample strains due to grain coarsening.

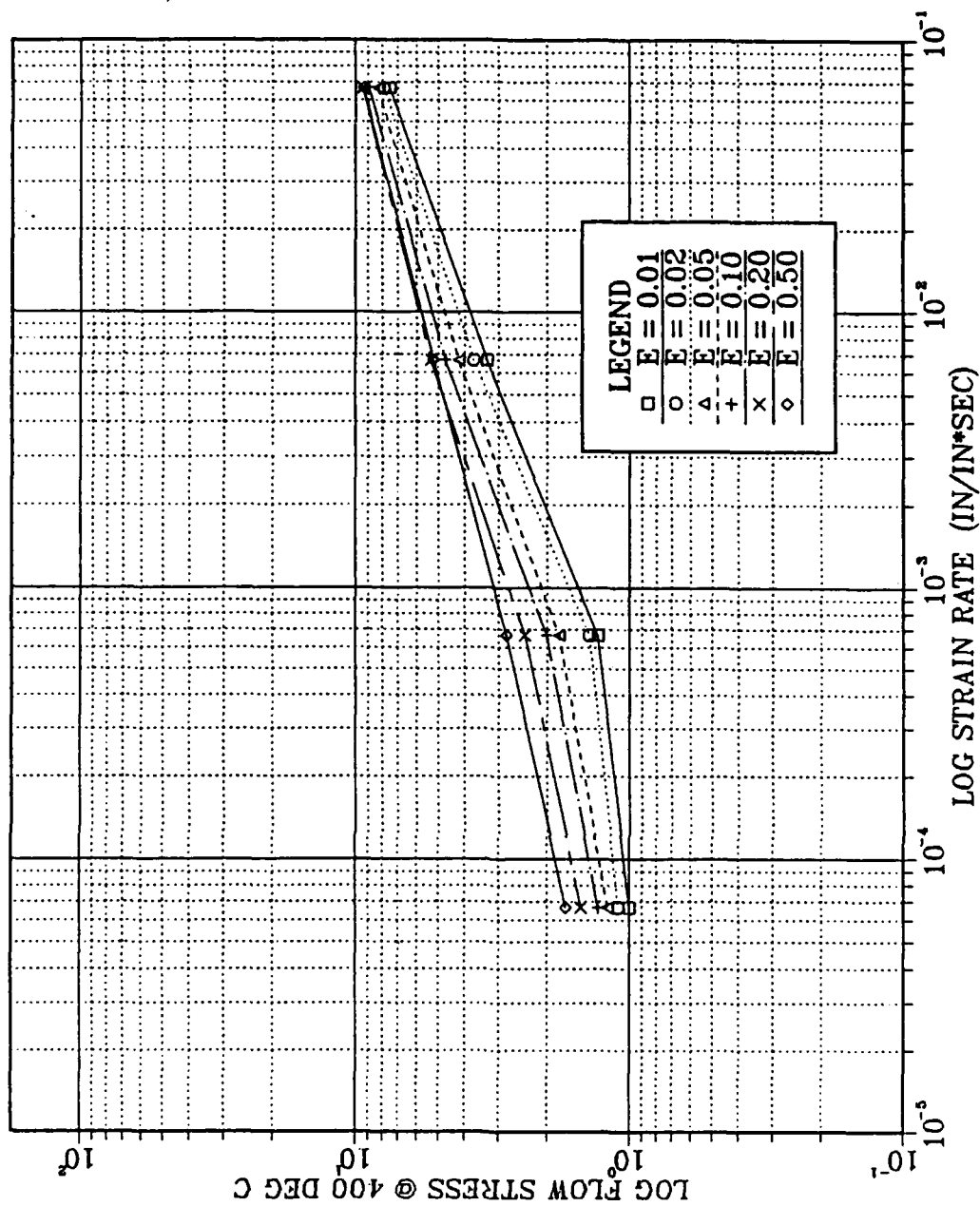


Figure 45. TMP C Variation of strain rate sensitivity: Strain rate sensitivity varies as the sample strains due to grain coarsening.

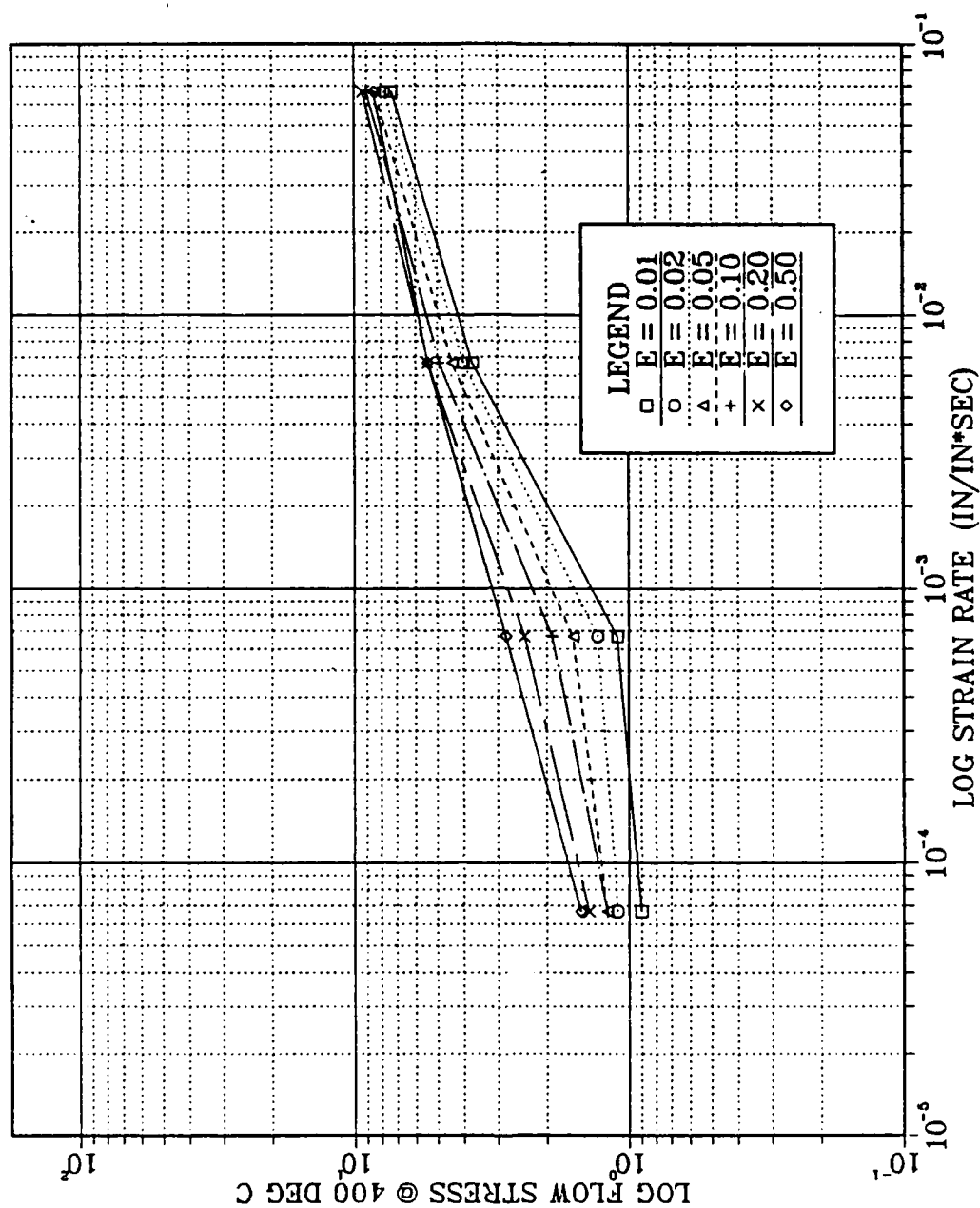


Figure 46. TMP D Variation of strain rate sensitivity: Strain rate sensitivity varies as the sample strains due to grain coarsening.

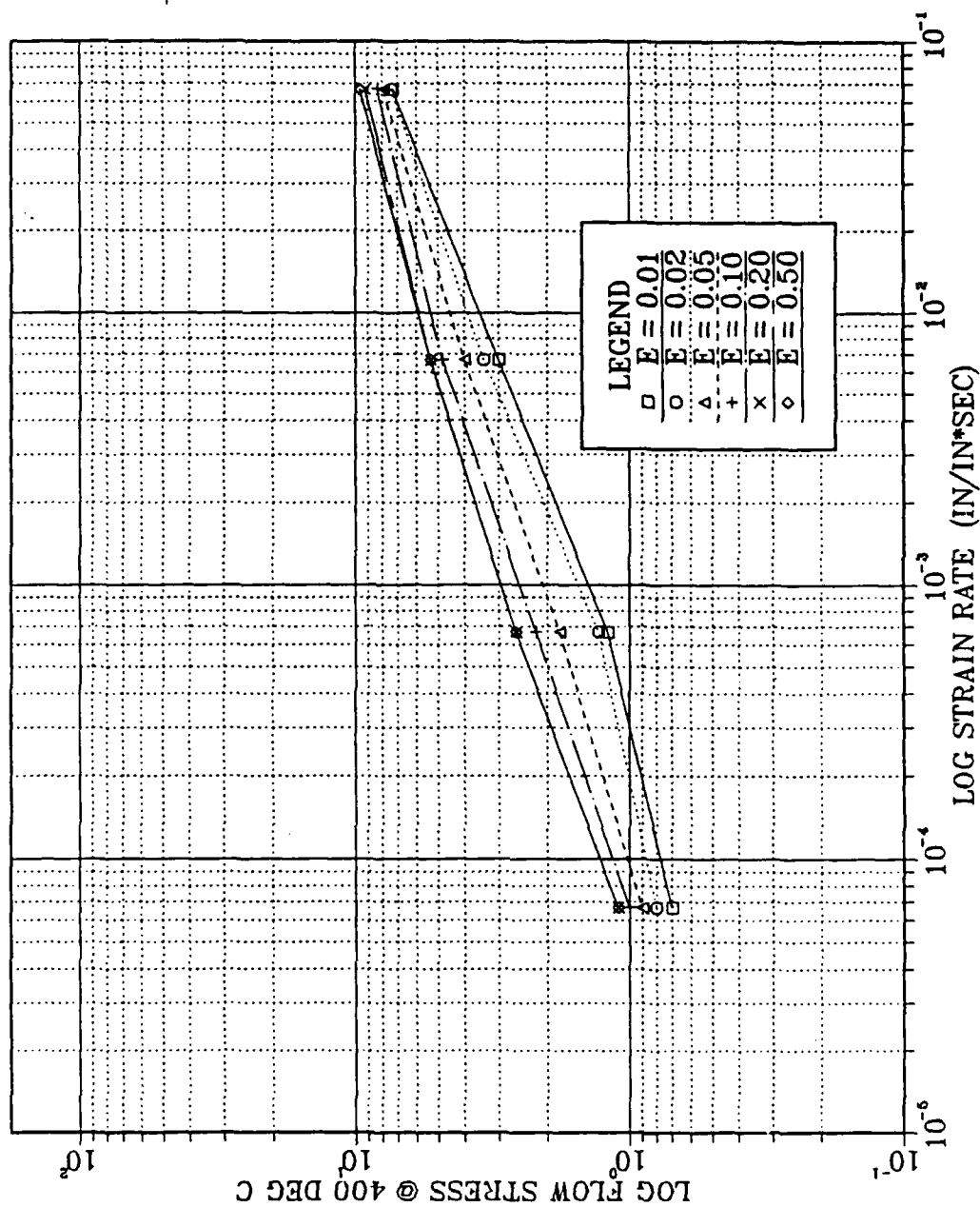


Figure 47. TMP E Variation of strain rate sensitivity: Strain rate sensitivity varies as the sample strains due to grain coarsening.

LIST OF REFERENCES

1. Hamilton, C. H. and Stacher G. W., "Superplastic Forming of Ti-6Al-4V Beam Frames," *Metal Progress*, pp.34-37, March, 1976.
2. Hatch, J. E., *Properties and Physical Metallurgy*, pp. 51,338, American Society for Metals, 1984.
3. Mondolfo, L. F., *Aluminum Alloys: Structure and Properties*, pp. 554-556, Butterworths, London, 1976.
4. Thompson, G. E. and Noble, B., "Precipitation Characteristics of Aluminum-Lithium Alloys Containing Magnesium," *Journal of the Institute of Metals*, v. 101, pp. 111-115, March, 1973.
5. Lee, E. -W., Divecha D. and Karmarkar S, "The Effect of Cu Content and Amount of Cold Work on the Mechanical Properties of NAVALITE," *Lightweight Alloys for Aerospace Application*, Lee, E. -W., Kim, N. J. and Chia, H. L. (eds.), TMS-AIME, in press, 1989.
6. *Metals Handbook*, 9th Ed., v. 2, p.130, American Society for Metals, 1986.
7. Sherby, O. D. and Wadsworth, J., "Development and Characterization of Fine-Grain Superplastic Materials," *Deformation, Processing and Structure*, pp. 364-369, American Society for Metals, 1982.
8. Hales, S. J. and others, "Grain Refinement and Superplasticity in a Lithium-Containing Al-Mg Alloy by Thermomechanical Processing," *Journal de Physique*, Colloque C3, Supplement au n°9. Tome 48, September, 1987.
9. Hales, S. J. and McNelley, T. R., "Microstructural Evolution by Continuous Recrystallization in a Superplastic Al-Mg Alloy," *Acta Metall.*, v. 36, pp. 1229-1239, 1988.

10. Nix, W. D., "On Some Fundamental Aspects of Superplastic Flow," S. P. Agrawal (ed), *ASM*, p. 3, 1984.
11. Hales, S. J. and McNelley, T. R., "Fine Grained Superplasticity at 300°C in a Wrought Al-Mg Alloy", *Superplasticity in Aerospace*, Heikkinen, H. C. and McNelley, T. R. (eds.), p.61, TMS-AIME, Warrendale, PA, 1988.
12. Lee, E. -W. and McNelley, T. R., "Microstructure Evolution during Processing and Superplastic Flow in a High Magnesium Al-Mg Alloy," *Materials Science and Engineering*, v. 93, pp. 45-55, 1987.
13. Munroe, I. B., *Optimizing Superplastic Response in Lithium Containing Aluminum-Magnesium Alloys*, Master's Thesis, Naval Postgraduate School, Monterey, California, 1987.

INITIAL DISTRIBUTION LIST

		No. Copies
1.	Defense Technical Information Center Cameron Station Alexandria, VA 22304-6145	2
2.	Library, Code 0142 Naval Postgraduate School Monterey, CA 93943-5002	2
3.	Naval Engineering Curricular Office, Code 34 Naval Postgraduate School Monterey, CA 93943	1
4.	Professor T. R. McNelley, Code 69.Mc Department of Mechanical Engineering Naval Postgraduate School Monterey, CA 93943	5
5.	Dr. Eui-Whee Lee, Code 6063 Naval Air Development Center Warminster, PA 18974	1
6.	Dr. Lewis E. Slotter, Code AIR 931A Headquarters, Naval Air Systems Command Washington, D.C. 20361	1
7.	LT Alden P. Chester, III 716 Prince Charles Lane Virginia Beach, VA 23452	2